VTT PUBLICATIONS 387

Ignition of and fire spread on cables and electronic components

Olavi Keski-Rahkonen & Johan Mangs

VTT Building Technology

Antti Turtola

VTT Automation

TECHNICAL RESEARCH CENTRE OF FINLAND
ESPOO 1999

ISBN 951–38–5385–3 (soft back ed.)
ISSN 1235–0621 (soft back ed.)

ISBN 951–38–5386–1 (URL: http://www.inf.vtt.fi/pdf/)
ISSN 1455–0849 (URL: http://www.inf.vtt.fi/pdf/)

JULKAISIJA – UTGIVARE – PUBLISHER

Valtion teknillinen tutkimuskeskus (VTT), Vuorimiehentie 5, PL 2000, 02044 VTT
puh. vaihde (09) 4561, faksi (09) 456 4374

Statens tekniska forskningscentral (VTT), Bergsmansvägen 5, PB 2000, 02044 VTT
tel. växel (09) 4561, fax (09) 456 4374

Technical Research Centre of Finland (VTT), Vuorimiehentie 5, P.O.Box 2000, FIN–02044 VTT, Finland
phone internat. + 358 9 4561, fax + 358 9 456 4374

VTT Rakennustekniikka, Rakennusfysiikka, talo- ja palotekniikka, Kivimiehentie 4, PL 1803, 02044 VTT
puh. vaihde (09) 4561, faksi (09) 456 4815

VTT Byggnadsteknik, Byggnadsfysik, hus- och brandteknik, Stenkarlsvägen 4, PB 1803, 02044 VTT
tel. växel (09) 4561, fax (09) 456 4815

VTT Building Technology, Building Physics, Building Services and Fire Technology,
Kivimiehentie 4, P.O.Box 1803, FIN–02044 VTT, Finland
phone internat. + 358 9 4561, fax + 358 9 456 4815

VTT Automaatio, Tuotetekniikka, Otakaari 7 B, PL 13051, 02044 VTT
puh. vaihde (09) 4561, faksi (09) 456 7042

VTT Automation, Produktteknik, Otsvängen 7 B, PB 13051, 02044 VTT
tel. växel (09) 4561, fax (09) 456 7042

VTT Automation, Product Technology, Otakaari 7 B, P.O.Box 13051, FIN–02044 VTT, Finland
phone internat. + 358 9 4561, fax + 358 9 456 7042

Technical editing Kerttu Tirronen

Libella Painopalvelu Oy, Espoo 1999

Keski-Rahkonen, Olavi, Mangs, Johan & Turtola, Antti. Ignition of and fire spread on cables and electronic components. Espoo 1999. Technical Research Centre of Finland, VTT Publications 387. 102 p. + app. 10 p.

Keywords ignition, fire safety, fire propagation, fire protection, cables, electric devices, electrical components, conduction, heat transmission, self ignition, short and ground circuits, arcs

ABSTRACT

This paper reviews electrical ignition phenomena from a wide perspective through statistical, modelling and experimental tools. A rather comprehensive concept of electrical ignition phenomena has been described. Several databases indicate that defective cables leading to short circuit and ground shorts, as well as loose connections leading to overheating, are the most common reasons for electrical ignitions. For modelling an overheated cable a mathematical model has been proposed, which compares favourably with a limited set of experimental data. Experiments on PVC cables showed self-heating a possible but improbable cause of initial ignition. The literature review of physical models of electrical arcs established conditions where ignition of cables might be possible. A limited set of tests under poorly controlled conditions succeeded, not producing long lasting arcs amenable to sustained ignition. The reason for experimental failure is believed to be too violent release of energy, which blew off the flames.

Existing semiquantitative models of flame spread are shown to be able to describe salient features of cable ignitions despite clear deviations of the initial assumptions of the model. Laboratory tests of electronic components heavily or destructively overloaded did not generally lead to ignition of adjacent material because of sudden release and subsequent destruction of the component. Only power transistors heavily mounted on printed cards seemed able to start ignition of the card. The phenomenon can be modelled as a piloted ignition similar to flame spread on cables.

PREFACE

This study was carried out as a part of the Fire Safety Project (PALOTUB) which is one of the projects in the Research Programme on the Structural Integrity of Nuclear Power Plants (RATU 2).

The study has been financed by the Finnish Centre for Radiation and Nuclear Safety, the Ministry of Trade and Industry, IVO Power Engineering Ltd, Teollisuuden Voima Oy and the Finnish Fire Research Board.

We are indebted to J. Björkman, H. Juutilainen and K. Taimisalo (VTT Building Technology), as well as H. Palmén (VTT Automation) for help in several of the experiments described here.

CONTENTS

1 INTRODUCTION

Electrical ignition accounts for a large proportion of initial sources of fires in the statistics of many countries. Any source of energy which could be released if uncontrolled may create the conditions to start a fire. Despite this commonness, there is not very much literature available which describes ignitions of electrical origin as physical phenomena, using the scientific and technical tools we have currently available.

The purpose of this work was to establish quantitative and semiquantitative estimates and methods to assess electrical ignition processes, considering especially electronic components used in nuclear power plants. Three methods were used to approach the problem: literature study of available statistical data, modelling of ignition phenomena, and qualifying them against simple small-scale experiments. The application of results was to facilitate estimating ignition thresholds for electrical and electronic equipment for fire PSA in nuclear power plants.

There are not many treatises in literature to address specifically cable ignitions in nuclear power plants. Ivannikov and Zernov (1990) wrote an electrotechnical approach but remained at such a general level, it does not lend much to detailed applications.

2 LITERATURE REVIEW ON ELECTRICAL IGNITION SOURCES

There is little published information about specific electrical ignition sources. The information available is usually on a quite general level, and the division into different groups of electrical causes is not unequivocal.

It should also be noted that a failed electrical component is not necessarily the first ignited component or material, although this is so in many cases. The original electrical failure may occur in one device inducing other electrical faults in nearby electrical devices, finally leading to fire. The chain of different faults may consist of several phases.

The original electrical fault may also produce enough heat to directly ignite combustible material in the vicinity. An ignition mechanism associated with oil-filled devices such as transformers includes rupture of the device followed by ignition of the dispersed combustible oil by e.g. arcs, sparks or hot surfaces.

The distinction between electrical ignition mechanism, failed electrical component and first ignited combustible material/component is not always clear in the literature, which introduces uncertainty in the statistics.

2.1 STATISTICS ON ELECTRICAL FAULTS IN GENERAL

Here, some general information on electrical fire causes is first presented. Although these fires are not explicitly connected to electrically induced fires in nuclear power plants, electricity as a physical phenomenon remains the same, and some general conclusions can be drawn.

2.1.1 Statistics from Finland

Fires recorded as electrically induced were collected from statistics on large fire accidents in Finland 1980 - 1993 based on unpublished material from the Federation of Finnish Insurance Companies. A fire accident was recorded as large if the value of the damage exceeded 0.25 Mmk in 1980, 0.5 Mmk 1981 - 1985 and 1.0 Mmk 1986 - 1993. The fire targets varied

and included industrial, residential, agricultural, educational etc. objects. Ignition mechanism and failed component were used without distinction in these statistics to express fire cause and the results are presented in Figure 1. Fire causes denoted as “electrical device” or “electrical” without further specification amount to 42% of the cases, giving an indication of the uncertainty of the statistics.

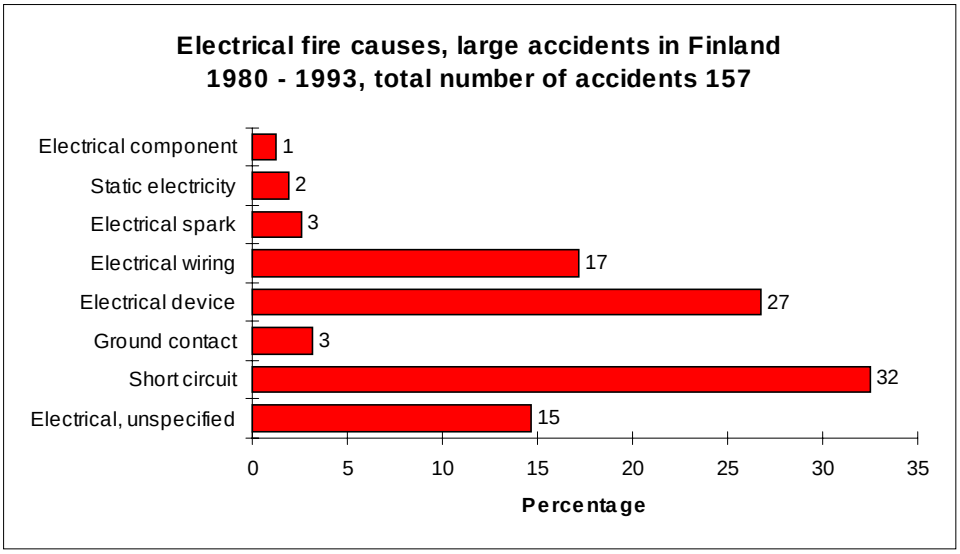

Figure 1. Electrical fire causes recorded from large accidents in Finland 1980 - 1993. Total number of accidents in this figure is 157.

The causes of electrical fire and the total number of fires in Finland during 1994 and 1995 as recorded in the Finnish national accident data base ONTIKA are presented in Table 1. The data base ONTIKA contains information on accidents which concern the fire and rescue authority. The fire officer in command at the fire scene is responsible for collecting information about the accident for ONTIKA. The fire cause recorded is often only a rough guess because the fire brigade do not perform fire investigations. This concerns especially cases where the fire cause is not obvious, as in many fires of electrical origin.

Table 1. Fire causes in Finland in 1994 and 1995 according to Finnish national accident data base ONTIKA (Tamminen 1996).

Fire cause	**1994**		**1995**	
	number	**%**	**number**	**%**
Electrical fires				
Short circuit or ground fault	870	75	984	72
Loose connection	36	3	56	4
Overheating	54	5	73	5
Improper installation	17	1	11	1
Other electrical faults	186	16	236	17
Electrical faults, total	**1163**	**100**	**1360**	**100**
All fires				
Electrical faults, total	1163	13	1360	13
Lightning	287	3	306	3
Other known causes	6229	70	6798	67
Unknown	1191	13	1580	16
Total	**8870**	**100**	**10044**	**100**

2.1.2 Statistics from the USA

The distribution of electrical fires between different products in the USA in 1990 is presented in Table 2. The most frequent is electrical cooking equipment, reported as fire cause in 38% of the total. This is probably misleading because ignition of oil, fat or other combustible products near the hot cooking appliance is responsible for a considerable number of cooking equipment fires. They are thus not truly electrical in origin.

The second type of equipment is electrical distribution, responsible for fire in 28% of total.

Table 2. Estimated fire losses in residential structural electrical fires in the USA, by kind of equipment (eq.) involved, 1990 (U.S. Consumer product safety commission 1992). Columns do not add to total due to rounding.

Electrical product	Fires (number)	Fires (%)	Property loss (M$)	Property loss (%)
Heating eq.	10100	7	76.1	6
Cooking eq.	56900	38	224.3	19
Electrical distribution	42000	28	568.5	47
Cooling eq.	4500	3	36.2	3
Appliances	20800	14	157.8	13
Other eq.	1500	1	10.4	1
Unknown eq.	16700	11	164.8	14
Total electrical	149900	100	1208.4	100

As an example of the distribution of different electrical fire causes in some specific electrical apparatus, data on televisions, radios, video cassette recorders and phonographs due to fire statistics in the USA 1988 - 1992 are considered in Figure 2 (Miller 1994). Of all appliances or tool fires, these accounted for the largest number of civilian fire deaths and were placed third in number of civilian fire injuries and pecuniary loss.

Short circuit or ground fault was the leading cause of these home fires, accounting for nearly 48% of the fires and between 44 and 48% of associated losses. Electrical wire or cable insulation was the leading form of material first ignited in television, radio, video cassette recorder and phonograph fires, civilian fire deaths and direct property damage. Appliance housing or casing was the second leading form of material first ignited.

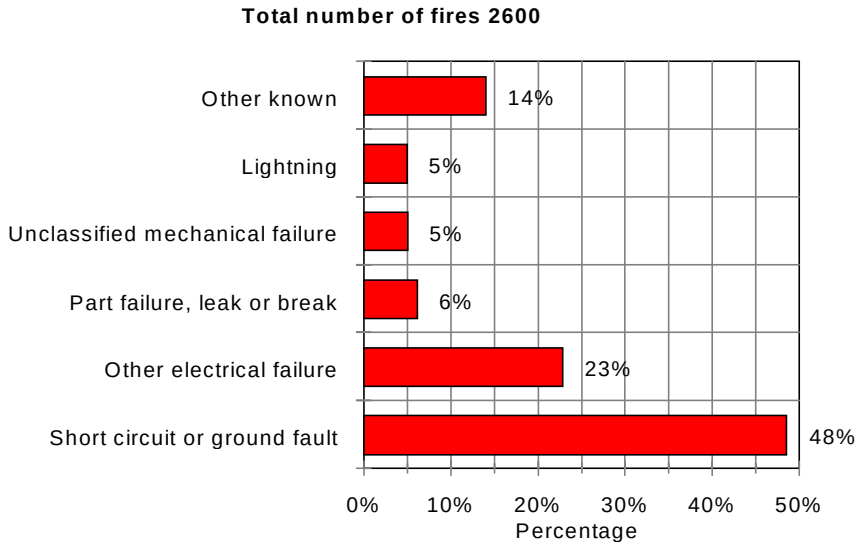

Figure 2. Distribution of different electrical fire causes in television, radio, video cassette recorder and phonograph fires due to fire statistics in the USA 1988 - 1992, annual average (Miller 1994).

2.1.3 Analysis of electrical fire investigation in ten cities

Gomberg and Hall (1983) describe 110 detailed electrical fire investigations from 10 cities in the USA. Most cases were single family dwellings (84%), with the remainder either duplexes or small apartments (up to six units). The fire cases are tabulated in the report using different parameters. The analysis is not extended to the physical processes leading to ignition, neither are ignition probabilities presented in the report. The failure mode by component in these 100 fire cases is presented in Table 3. The components are divided into six groups for clarity. Altogether 12% were denoted "failure mode unknown".

The following areas were pointed out in the conclusions to be examined further:

(1) the factors that cause *overcurrent protection* devices to fail to operate
(2) the role of extension cords *misused* as permanent extensions of basic wiring as the apparent dominant factor in fires involving cord and plugs
(3) the problem of *loose connections* between receptacle and wiring, which appears to be the leading failure mode for receptacle fires.

Table 3. Failure mode by component in 110 electrical fires in the USA (Gomberg and Hall 1983).

		Number	Percentage
Service components (utility supply conductors, service entrance wiring, service equipment, distribution panel)			
– deteriorated insulation		5	5
– improper installation => ground fault or overloading		4	4
– alterations in progress, e.g. accidental contact with high voltage line, removal of support for service entrance cable		2	2
– unknown		4	4
	total	15	14
Branch circuit wiring			
– mechanical damage or improper installation		9	8
– poor or loose splice		8	7
– ground fault		4	4
– use of improper wiring		3	3
– knob and tube encapsulated		3	3
– miscellaneous overload		2	2
– unknown		3	3
	total	32	29
Cords and plugs			
– mechanical damage or poor splice		11	10
– overloaded extension cord		6	5
– overloaded plug		2	2
– damaged plug		2	2
– short, water, deteriorated insulation, electric blanket cord		6	5
– unknown		1	1
	total	28	25
Receptacles and outlets			
– loose or poor connection		8	7
– mechanical damage		3	3
– overloaded		2	2
– deteriorated, miswired, plug inserted improperly		3	3
– unknown		4	4
	total	20	18
Lamp and lighting fixtures			
– loose or poor connection or splice, miswiring		5	5
– combustibles too close		5	5
– overlamped		3	3
– deteriorated insulation		1	1
	total	14	13
Low voltage transformer		1	1
	total	1	1
	total of investigated cases	**110**	**100**

2.1.4 Statistics from Russia

The assessment of electrical fire risk and fire hazard probability in Russia has been discussed by Smelkov & Pekhotikov (1996, 1997), Smelkov et al. (1995), and Smelkov (1992, 1993). The articles concern the estimation of fire safety of different electrotechnical commercial products and present general principles using the standard IEC 695-1-1 as a basic document.

In the articles the following formula is presented for calculations

$$Q_f = Q_{fc} * Q_{fv} * Q_{pf} * Q_{ign} < 10^{-6} \quad (1)$$

where

Q_{fc} is the probability of characteristic fire hazardous conditions occurring in one of the parts of the product per year (short circuit, overload etc.)

Q_{fv} is the probability that the characteristic electrotechnical parameter (current, transient resistance, etc.) lies in the range of fire hazardous values

Q_{pf} is the probability of protective gear failure

Q_{ign} is the probability that the combustible material attains the critical temperature or ignites.

An admissible fire risk has been specified in Equation (1) to be 10^{-6} per year. The probabilities in Equation (1) are defined in the articles and some algorithms are presented. No examples or numbers on specified electrical items or components are presented. Some tables on the distribution of fires as to types of products are presented. For example, in 1996, 293 507 fires occurred in Russia of which 20.5% were of electrical origin (Smelkov & Pekhotikov 1997). The four leading types of products causing electrical fires are presented in Table 4.

Table 4. The four leading types of products causing electrical fires in Russia 1996 (Smelkov & Pekhotikov 1997).

Product type	Number of fires	Percentage
Cable, wire	35247	58.6
Electrical fire place	6776	11.3
Television set	4033	6.7
Switchboard	3009	5.0
Other types of products	11069	18.4

2.1.5 Discussion

Despite the number of unknown fire causes and possibly different criteria for classifying fire causes in the above presented databases the following similarities can be noted:

The leading ignition mechanism recorded is short circuit/ground fault (Figures 1 and 2 and Table 1). Gomberg and Hall (1983) point out loose connections between receptacle and wiring to be the leading failure mode of receptacle fires.

Considering specified components, electrical wiring is mentioned as 17% in Figure 1 and electrical distribution as 28% in Table 2. The majority of components in Table 3 are wiring and components connected to wiring such as splices, plugs, receptacles and outlets. Cable or wire is also pointed out in Table 4 as the most frequent type of product causing electrical fires.

2.2 SANDIA NATIONAL LABORATORIES NUCLEAR POWER PLANT FIRE EVENT DATA BASE

2.2.1 Background

The Sandia National Laboratories (SNL) Nuclear Power Plant Fire Event Data Base catalogues fire events occurring in U.S. commercial nuclear power plants as reported to the U.S. Nuclear Regulatory Commission (USNRC) and in some cases to insurance companies. The data contain descriptions as provided in the original event reports. The data represent the whole U.S. nuclear power industry.

There are two versions of the data base available. The original 1985 - 1986 published version covered events from 1965 through June 1985 (Wheelis 1986). In 1993 - 1994 the data base was updated, although it was never published. The update has nonetheless been placed in the USNRC public document room and is also publicly available.

The original data base contains 356 and the extension contains 97 fire events.

In the present work, descriptions of fires of electrical origin were collected from the fire event data base. The original data base included 81 and the extension 55 fires of electrical origin, altogether 136 electrical fires.

2.2.2 Results from SNL database

The reports were searched for the ignition mechanisms and the failed component in these electrical fire events and these are presented in Tables 5 and 6, respectively.

The aim was here to identify the actual component where the electrical malfunction initiating a sequence of events resulting in fire occurred. For example, in the case of electrical motors the “failed component” tabulated, if known, could be a switch, connector, wiring etc. If no specification was made in the data base report and only “electrical motor fire” was reported, the failed component was denoted “unknown”.

The failed component in electrical fires relating to different modes of plant operation is presented in Table 7.

The failed component in electrical fires relating to different plant locations is presented in Table 8.

The fire incidents during the construction phase were separated and categorised in a similar way. The results, ignition mechanism and failed component are presented in Tables 9 and 10.

The fire event descriptions in the SNL database are mostly limited and the true root cause is often missing, e.g. many causes are only mentioned as “electrical fault”. The ignition mechanism could therefore not be identified from the reports in 54% of the fire event descriptions. The first failed component or item was somewhat more carefully reported, but it was still unknown in 18% of the electrical fire events. The first material

ignited was not described in 68% of the events. The leading identified material first ignited was cable, wiring or bus insulation, 12% of the events.

It is to be noted that the term "unknown" in the tables refers to an unknown electrical fault or component and not to a totally unknown item.

Table 5. Ignition mechanisms in electrical fires in US nuclear power plants 1965 - 1989 (SNL database).

	Initial database		Updated part		Total	
Ignition mechanism	**Number**	**%**	**Number**	**%**	**Number**	**%**
Overheating	6	7	10	18	16	12
Short	16	20	7	13	23	17
Ground fault	3	4	2	4	5	4
Arcing	8	10	2	4	10	7
Loose connections	7	9	1	2	8	6
Static electricity	1	1	0	0	1	1
Unknown	40	49	33	60	73	54
Total	81	100	55	100	136	100

Table 6. Failed component in electrical fires in US nuclear power plants 1965 - 1989 (SNL database).

	Initial database		Updated part		Total	
Failed component	**Number**	**%**	**Number**	**%**	**Number**	**%**
Cable	10	12	3	5	13	10
Wiring	3	4	2	4	5	4
Bus	4	5	5	9	9	7
Switch, breaker	8	10	8	15	16	12
Contact, splice, terminal	12	15	7	13	19	14
Relay	5	6	14	25	19	14
Transformer	17	21	4	7	21	15
Resistor	1	1	1	2	2	1
Capacitor	1	1	2	4	3	2
Coil	1	1	0	0	1	1
Diode	0	0	1	2	1	1
Circuit card	0	0	1	2	1	1
Rotor in contact with stator	1	1	0	0	1	1
Unknown	18	22	7	13	25	18
Total	81	100	55	100	136	100

Table 7. Failed component in electrical fires in US nuclear power plants related to different modes of operation (SNL database).

Mode of operation	Total number	%	Cable, wiring, bus	%	Switch, breaker, relay	%	Contact, splice, terminal	%	Transformer	%	Components[1)]	%	Unknown	%
Construction	23	17	5	19	2	6	3	16	3	14	0	0	10	40
Cold shutdown	12	9	2	7	5	14	1	5	1	5	3	33	0	0
Hot shutdown	3	2	1	4	1	3	0	0	0	0	0	0	1	4
Shutdown	1	1	0	0	1	3	0	0	0	0	0	0	0	0
Power operation	69	51	14	52	18	51	10	53	12	57	5	56	10	40
Pre-operational testing	8	6	1	4	0	0	2	11	3	14	0	0	2	8
Maintenance outage	1	1	0	0	0	0	0	0	0	0	0	0	1	4
Refueling outage	9	7	1	4	4	11	2	11	1	5	0	0	1	4
Not mentioned	10	7	3	11	4	11	1	5	1	5	1	11	0	0
Total	136	100	27	100	35	100	19	100	21	100	9	100	25	100

1) Components: 2 resistors, 3 capacitors, 1 coil, 1 diode, 1 circuit card and 1 rotor in contact with stator

Table 8. Failed component in electrical fires related to different locations in US nuclear power plants (SNL database).

Location	Number	%	Cable, wiring, bus	Switch, breaker, relay	Contact, splice, terminal	Transformer	Components[1)]	Unknown
Auxiliary Building	14	10	4	3	2	1	2	2
Battery Room	3	2			2		1	
Block House	1	1	1					
Cable Riser Area	2	1			2			
Cable Spreading Room	3	2	2	1				
Containment	3	2	1					2
Control Building	7	5		4	1			2
Control Room	8	6		5			3	
Cooling Tower	2	1	1		1			
Diesel Generator Building	4	3		1			1	2
Fire Pump House	1	1			1			
Offsite	1	1				1		
Other Building	14	10	1	5	1	4		3
Pump Room	2	1						2
Radwaste Building	1	1						1
Reactor Building	8	6	1	4				3
Service Building	1	1		1				
Switchgear Room	9	7	3	4	1	1		
Temporary Building	5	4	1		1			3
TIP Room	1	1			1			
Transformer Yard	21	15		3	4	12	1	1
Turbine Building	11	8	7		1	2		1
Warehouse	1	1	1					
Yard	2	1	1					1
Not mentioned	11	8	3	4	1		1	2
Total	136	100	27	35	19	21	9	25

[1)] Components: 2 resistors, 3 capacitors, 1 coil, 1 diode, 1 circuit card and 1 rotor in contact with stator

Table 9. Ignition mechanisms in electrical fires in US nuclear power plants under construction 1965 - 1989 (SNL database).

Ignition mechanism	**Number**	**%**
Overheating	1	4
Short	6	26
Ground fault		0
Arcing	2	9
Loose connections	1	4
Static electricity		0
Unknown	13	57
Total	23	100

Table 10. Failed component in electrical fires in US nuclear power plants under construction 1965 - 1989 (SNL database).

Failed component	**Number**	**%**
Cable	3	13
Wiring	2	9
Bus		0
Switch, breaker	2	9
Contact, splice, terminal	3	13
Relay		0
Transformer	3	13
Resistor		0
Capacitor		0
Coil		0
Diode		0
Circuit card		0
Unknown	10	43
Total	23	100

2.2.3 Discussion

Ignition mechanism

The great number of cases with unknown ignition mechanisms (54%) introduce a considerable amount of uncertainty in Table 5. Short circuit is the leading recorded mechanism (17%), followed by overheating (12%), arcing (7%) and loose connections (6%).

Failed component

The failed component in Table 6 is usually a switch, breaker or relay (26%), i.e. a component with movable mechanical parts. Cable, wiring or bus accounts for 21% of the cases and contacts, splices and terminals, which are usually connected to cable or wiring, account for 14%. Transformers also constitute a frequent group (15%). Miscellaneous components such as resistors, capacitors, coils, diodes or circuit cards account for only 6% of the cases. Also here, the unknown component constitutes a considerable part of the statistics (18%).

2.3 IAEA AND OECD/NEA AIRS DATABASE EVENTS ON ELECTRICAL FIRES

2.3.1 Background

The Incident Reporting System (IRS) is an international system maintained jointly by the Nuclear Energy Agency (NEA) and the International Atomic Energy Agency (IAEA) for the promotion of safety in the nuclear power industry. Information is provided by participating countries on unusual events considered important for safety or accident prevention and action. The information is stored in a database.

The database used here is the October 1997 release of version 1.1 of the Advanced Incident Reporting System (AIRS) Database (International Atomic Energy Agency 1997). It was provided by the Finnish Radiation and Nuclear Safety Authority (STUK) on the condition of confidentiality. The database contained 2591 reports describing incidents from the period 1974 - 1997. The corresponding total number of reactor years is 8656 [1].

[1] D. Ruatti, IAEA, private communication 7.5.1998.

Electrically induced fires were sought using the “Free form search” method for the word “fire” in the event reports in the AIRS database. This search gave 275 documents containing “fire” or a variant of it obtained by stemming. These 275 reports were read through and 34 reports describing 39 fires originating from electrical faults were found. The electrical fire incidents described occurred in the period 1981 - 1996.

The description of what actually happened in the electrical circuits is incomplete in many of the reports, leaving the failure mechanism and failed and/or ignited component unspecified. In some cases where fire causes are presented they are described as “possible” or “supposed”.

As mentioned before, the failed electrical component is not necessarily the first ignited component or material. The original electrical failure may occur in one device inducing other electrical faults in nearby electrical devices and finally leading to fire. The chain of different faults may consist of several phases, as was the case in some of the AIRS-reported events.

2.3.2 Results from AIRS database

Electrical failure mechanisms leading to ignition are presented in Table 11, failed electrical components in Table 12 and first ignited component or material in Table 13.

All unspecified or unclear mechanisms or components have been grouped as “unknown”.

It is to be noted that the term “unknown” in the tables refers to an unknown electrical ignition mechanism or component and not to a totally unknown item.

Table 11. Failure mechanism leading to ignition in fires originating from electrical faults as described in AIRS event reports.

Failure mechanism	**Number**	**%**
Overheating	5	13
Short	6	15
Ground fault	5	13
Arcing	7	18
Loose connections	3	8
Unknown	13	33
Total	39	100

Table 12. Failed component in fires originating from electrical faults as described in AIRS event reports.

Failed component	**Number**	**%**
Cable	4	10
Switch, breaker	10	26
Contact, splice, terminal	6	15
Relay	2	5
Transformer	10	26
Slip ring in turbogenerator	1	3
Unknown	6	15
Total	39	100

Table 13. Ignited component or material in fires originating from electrical faults as described in AIRS event reports.

Ignited component	Number	%
Cable insulation	8	21
Switch, breaker	4	10
Contact, splice, terminal	1	3
Relay	2	5
Oil	11	28
Slip ring in turbogenerator	1	3
Unknown	10	26
No fire spread[*)]	2	5
Total	39	100

[*)] Two cases: 1. scorching of cable insulation and risk of fire
2. the electrical fault was interrupted within a few seconds by the over-current protection

2.3.3 Discussion

As mentioned above, there is a significant degree of uncertainty in investigations of electrical faults. The ignition mechanism is unknown in 33% of the events, the failed component is unknown in 15% and the ignited component is unknown in 26% of the AIRS-event reports.

Among recognized *ignition mechanisms* arcing (18%), short circuit (15%), overheating (13%) and ground fault (13%) are about equally frequent. Loose connections are mentioned in 8% of the events.

The *failed component* is usually a switch, breaker or relay (31%), i.e. a component with movable mechanical parts. The most frequent single component is a transformer (26%).

The most frequent *first ignited component or material* is oil (28%) corresponding to a transformer as the most frequent single failed component. The second ignited component is cable insulation (21%). Cable was mentioned as a failed component in 10% of the cases. This reflects the cases where the original fault has occurred in a switch,

breaker, contact, terminal etc. igniting insulation of connected or nearby cable(s).

2.4 CONCLUSIONS FROM STATISTICS ON ELECTRICAL IGNITION SOURCES

The large number of electrical fire causes recorded as unspecified electrical fault or appliance introduces uncertainty into the statistics. Further, many of the specified ignition mechanisms and failed components are presented as “possible” or “supposed”. This should be taken into account when interpreting the results.

The ignition and fire is in many cases the result of a chain of faults, raising difficulties in defining the true root cause. For example, a loose connection may induce overheating in the circuit leading to ignition of combustible material or the heating may destroy nearby insulation leading to short circuits or arcing. Overcurrent in a cable can in the same manner lead to either local overheating and ignition of combustible material or lead to insulation failure and arcing or short circuit.

Another factor concerning the usability of the databases is the presence or absence of events which did not result in a fire although the risk of fire did exist (precursor events). Such events cause e.g. electrical fuses or breakers to operate because of electrical over-current, smoke alarm, short circuits- etc. This absence of precursor events as well as poor identifying of true root causes has been pointed out by Madden (1997) concerning mainly Sandia and the Electric Power Research Institute (EPRI) fire event databases.

One can still draw some conclusions about electric ignition mechanisms, failed components and first ignited materials.

Ignition mechanisms

Generally, electrical ignition mechanisms can roughly be divided into four groups:

1. Short circuit, ground fault and arcing
2. Overheating

3. Loose connections
4. Static electricity.

The first group is the most frequent in SNL and AIRS databases (28 and 46%, respectively), while overheating (12 and 13%, respectively) and loose connections (6 and 8% respectively) are less frequently denoted as ignition mechanisms.

One interpretation of the relative occurrence of these mechanisms is the following. One of the reasons for short circuit, ground faults or arcing is insulation failure which can be due to several causes, one of which is overheating. This in turn can be due to electrical overloading or loose connections heating the insulation.

This is an example of a chain of electrical faults leading to fire. In the statistics, some of the fires attributed to short circuits, arcing or ground faults may thus have overloading or loose connections as initial electrical cause.

The static electricity case in Table 5 refers to a hydrogen gas explosion suspected to have been ignited by a spark caused by static electricity. Static electric discharges may ignite inflammable vapours, gases or dusts but not solid material.

The group of unknown electrical ignition mechanisms is notable (54% in SNL and 13% in AIRS database).

The same ignition mechanisms as above are also present in statistics on nuclear power plants in Germany, where less than one third of all fires were of electric origin[2]. There the most important mechanisms were: short circuit, ground contact, cables ignited after overloading, faulty solder joints and poor contacts between the pin and the socket in connectors.

The same mechanisms are also present in the statistics on electrical faults in general (section 2.1), with short circuit/ground fault as leading ignition mechanism followed by overheating and loose connections.

---

[2] M. Röwekamp, Gesellschaft für Anlagen- und Reaktorsicherheit (GRS) mbH. Private communication 1995.

Failed component

Three specific groups of critical components in nuclear power plants can be identified:

1. switches, breakers and relays
2. cables and contacts, splices and terminals
3. transformers.

Components such as circuit cards, resistors, capacitors, coils and diodes are responsible for a minor part of electrical fires in nuclear power plants.

The distribution of failed component related to different modes of operation shows a clear concentration on power operation (69%), followed by construction phase (23%).

The distribution of failed component related to different locations indicates transformer yards (21%) as a leading critical location followed by auxiliary building and unspecified ‘other building’ (14% each).

In the statistics on electrical faults in general (section 2.1) electrical cables and wiring, electrical distribution and components connected to wiring such as splices, plugs etc. are the most frequently specified components.

First ignited component or material

The first material ignited could be identified to a reliable extent in AIRS database only.

Oil from transformers, breakers, etc. is the leading material (28%) followed by cable insulation (21%). The ‘unknown’ group is also considerable here (26%).

Because the remaining components in Table 13 are connected to cables, one can draw the conclusion that cable insulation is the most important combustible material in the initial stage of electrically induced fires.

3 MODELLING THE HEATING OF AN INERT CABLE

For modelling ignition of an inert cable carrying an overload of current, we write a model describing the system as coupled heat conductors in cylindrical geometry. The principle of the geometric model is given in Figure 3, where the components and symbols are defined. The core cylinder is the metallic conductor (copper, aluminium) carrying the electric current. The outer cylinder is the insulator of the cable assumed to consist of only one homogenous, isotropic solid. Thermal and electric properties of the core and the insulator are assumed to be independent of temperature to allow for analytical solution of the problem to survey the time constants, and the heat transfer processes involved. The insulator is also assumed at this instant thermally inert, which means that even at elevated temperatures the insulator material does not react exothermically. We drop this requirement later when studying spontaneous ignition. For ignition of the surface of cable insulation material several extensive treatises are available (e.g. Vilyunov and Zarko 1989), but here we limit ourselves to modelling the heating of the insulator.

3.1 ENERGY SOURCE FROM THE CURRENT CONDUCTOR

Initially the cable is currentless at ambient temperature. At time $t = 0$ a current of density I'' is switched on, which creates a constant energy source density g in the conductor

$$g = I''^2 / \sigma \tag{2}$$

where σ is the resistivity of the conductor. The core and the insulator are assumed to be in perfect thermal contact with each other. This is not a good assumption, because during heating gaseous pyrolysis products are created which form gas pockets between the core and the insulator. The outer surface is cooled by convection and radiation, which is here modelled in a linear way by writing the cooling of temperature T_2 at the outer surface $r = b$

$$-k_2 \frac{\partial T_2(b,t)}{\partial r} = h_3 T_2(b,t); t > 0 \quad (3)$$

where h_3 is the linearized heat transfer coefficient including convection and radiation. Since both are functions of temperature, their values should be determined iteratively to represent the effective average value in the temperature range involved. The same rule applies to all other thermal and electrical properties, because in reality all of them depend to a certain degree on temperature.

3.2 HEAT CONDUCTION EQUATIONS

3.2.1 Basic heat conduction equations

Following standard texts, the heat conduction equations for the geometrical case described in Figure 3 can be written (Özisik 1980).

$$\alpha_1 \frac{1}{r}\frac{\partial}{\partial r}\left(r \frac{\partial T_1}{\partial r}\right) + \frac{\alpha_1}{k_1} g_1 = \frac{\partial T_1}{\partial t}; 0 < r < a, t > 0 \quad (4)$$

and

$$\alpha_2 \frac{1}{r}\frac{\partial}{\partial r}\left(r \frac{\partial T_2}{\partial r}\right) + \frac{\alpha_2}{k_2} g_2 = \frac{\partial T_2}{\partial t}; a < r < b, t > 0 \quad (5)$$

with initial condition

$$T_1(r,0) = T_2(r,0) = 0 \quad (6)$$

and boundary conditions

$$T_1(a,t) = T_2(a,t); t > 0 \quad (7)$$

$$-k_1 \frac{\partial T_1(a,t)}{\partial r} = -k_2 \frac{\partial T_2(a,t)}{\partial r}; t > 0 \quad (8)$$

including at the outer boundary the condition given by Equation (3) above.

Since the metal is a very good thermal conductor compared to the insulator, the temperature in the core is constant in the whole cross section. This approximation, allowing integration of Equation (4) over the volume of the core, simplifies the problem from one-dimensional composite medium to a single medium problem.

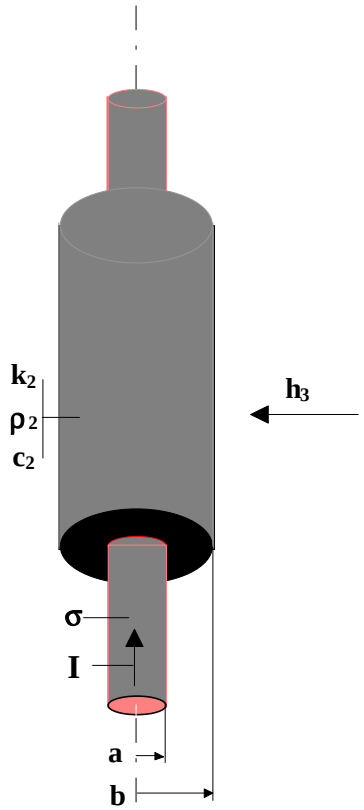

Figure 3. Geometry and notations of an insulated cable heated by electrical current.

3.2.2 Reduction to a single medium

Integrating Equation (3) in a volume element $dV = \pi a^2 dz$ over the whole core, one obtains

$$\int k_1 \frac{\partial^2 T_1}{\partial r^2} dV + \int \frac{k_1}{r} \frac{\partial T_1}{\partial r} dV + \int g_1 dV = \int c_1 \rho_1 \frac{\partial T_1}{\partial t} dV \quad (9)$$

where the thermal diffusivity $\alpha_1 = k_1 / c_1 \rho_1$ has been written out to correspond better to different energy transfer processes represented by the various terms in Equation (9). There are no temperature differences along the cable. We apply Equation (9) over the length element *dz* and the whole cross section

$$\int_0^a \frac{\partial^2 T_1}{\partial r^2} \cdot 2\pi k_1 r dr dz + \int_0^a \frac{k_1}{r} \frac{\partial T_1}{\partial r} \cdot 2\pi r dr dz + \int_0^a g_1 \cdot 2\pi r dr dz = \int_0^a c_1 \rho_1 \frac{\partial T_1}{\partial t} \cdot 2\pi r dr dz \quad (10)$$

Carrying out integrations bearing in mind that the functions do not depend on radius r leads to

$$2\pi k_1 dz \int_0^a \frac{\partial^2 T_1}{\partial r^2} \cdot r dr + 2\pi k_1 dz \int_0^a \frac{\partial T_1}{\partial r} \cdot dr + \pi a^2 g_1 dz = \pi a^2 c_1 \rho_1 \frac{\partial T_1}{\partial t} \cdot dz \quad (11)$$

Continuing integration term by term results in

$$2\pi k_1 dz \{ \Big/_0^a \frac{\partial T_1}{\partial r} \cdot r - \int_0^a \frac{\partial T_1}{\partial r} \cdot dr \} + 2\pi k_1 dz [T_1(a,t) - T_1(0,t)] + \pi a^2 g_1 dz = \pi a^2 c_1 \rho_1 \frac{\partial T_1}{\partial t} \cdot dz \quad (12)$$

The term in the brackets disappears because temperatures are the same throughout the cross section. The integral in the braces is the same as the

second integral in Equation (11) and disappears. Therefore, after substitutions

$$2\pi k_1 dz \cdot a \frac{\partial T_1}{\partial r}/_{r=a} + \pi a^2 g_1 dz = \pi a^2 c_1 \rho_1 \frac{\partial T_1}{\partial t} \cdot dz \tag{13}$$

Dividing by common factors and using boundary conditions (7) and (8) leads finally to

$$\frac{2}{a} \cdot k_2 \frac{\partial T_2}{\partial r}/_{r=a} + g_1 = c_1 \rho_1 \frac{\partial T_2}{\partial t}/_{r=a} \tag{14}$$

Collecting the results we get the mathematical problem in the form

$$\frac{\alpha_2}{r} \frac{\partial}{\partial r}\left(r \frac{\partial T_2}{\partial r} \right) = \frac{\partial T_2}{\partial t}; a < r < b, t > 0 \tag{15}$$

$$\frac{2k_2}{a} \cdot \frac{\partial T_2}{\partial r} + g_1 = c_1 \rho_1 \frac{\partial T_2}{\partial t}; r = a, t > 0 \tag{16}$$

$$k_2 \frac{\partial T_2}{\partial r} + h_3 T_2 = 0; r = b, t > 0 \tag{17}$$

$$T_2 = 0; a < r < b, t = 0 \tag{18}$$

3.2.3 Steady state solution

For a steady state temperature T_2^{∞} Equation (4) simplifies

$$\frac{\partial}{\partial r}\left(r \frac{\partial T_2^{\infty}}{\partial r} \right) = 0 \tag{19}$$

which integrates immediately to

$$T_2^{\infty} = C_1 \ln r + C_2 \tag{20}$$

where the integration constants C_1 and C_2 are determined from boundary conditions (17) and (18)

$$C_1 = -a^2 g_1 / 2k_2 \tag{21}$$

$$C_2 = \frac{a^2 g_1}{2bh_3}(1 + \frac{bh_3}{k_2} \ln b) \tag{22}$$

which substituted into Equation (20) gives

$$T_2^{\infty} = \frac{a^2 g_1}{2k_2}[\ln(\frac{b}{r}) + \frac{k_2}{bh_3}] \tag{23}$$

Denoting by T_0

$$T_0 = a^2 g_1 / 2k_2 \tag{24}$$

and the Biot number ***Bi*** by

$$\boldsymbol{Bi = bh_3/k_2} \tag{25}$$

the asymptotic temperature T_2^{∞}

$$T_2^{\infty} = T_0[1/Bi + \ln(b / r)] \tag{26}$$

3.2.4 Homogenisation of boundary conditions

Boundary condition (16) is nonhomogenous because of the source term g_1 but it can be homogenised by defining a new temperature variable $\vartheta(r,t)$

$$\vartheta(r,t) = T_2(r,t) - T_2^{\infty} \tag{27}$$

Substituting this into Equations (15 - 18) and arranging constants yields by straightforward calculation

$$\frac{1}{r}\frac{\partial}{\partial r}\left(r\frac{\partial \vartheta}{\partial r}\right) = \frac{1}{\alpha_2}\frac{\partial \vartheta}{\partial t}; a < r < b, t > 0 \tag{28}$$

$$-\frac{\partial \vartheta}{\partial r} - \frac{a c_1 \rho_1}{2 k_2}\frac{\partial \vartheta}{\partial t} = 0; r = a, t > 0 \tag{29}$$

$$\frac{\partial \vartheta}{\partial r} + \frac{h_3}{k_2}\vartheta = 0; r = b, t > 0 \tag{30}$$

$$\vartheta = -T_0[1/Bi + \ln(b/r)]; a < r < b, t = 0 \tag{31}$$

3.2.5 Separation of variables

For solving the modified heat conduction problem presented by Equations (28-31) the variables can be separated by defining

$$\vartheta(r,t) = \Psi(r)\Gamma(t) \tag{32}$$

Substituting these into Equation (28) and separating variables we get

$$\frac{1}{r\Psi_n}\frac{d}{dr}\left(r\cdot\frac{d\Psi_n}{dr}\right)=\frac{1}{\alpha_2\Gamma_n}\frac{d\Gamma_n}{dt}=\beta_n^2 \tag{33}$$

Since the first term on the left hand side depends only on r, and the second term on *t*, both must be constants, which we have denoted by β_n^2.

Substituting this proposal into Equation (28), and the equations defining boundary and initial conditions (29-31) yields for the eigenfunctions Ψ_n a Helmholtz equation

$$\frac{1}{r}\frac{d}{dr}\left(r\frac{d\Psi_n}{dr}\right)+\beta_n^2\Psi_n=0; a<r<b, n=1,2,3,\ldots \tag{34}$$

$$-\frac{d\Psi_n}{dr}-\frac{ac_1\rho_1\alpha_2\beta_n^2}{2k_2}\Psi_n; r=a \tag{35}$$

$$\frac{d\Psi_n}{dr}+\frac{h_3}{k_2}\Psi_n=0; r=b \tag{36}$$

and for Γ_n

$$\frac{d\Gamma_n}{dt}+\alpha_2\beta_n^2\Gamma_n=0, n=1,2,3\ldots \tag{37}$$

with an initial condition

$$\Gamma_n=1, t=0 \tag{38}$$

These last equations have an immediate solution

$$\Gamma_n = \exp(-\alpha_2 \beta_n^2 t) \tag{39}$$

The spatial eigenfunctions are expressed in terms of zero order Bessel functions of the first kind J_0 and the second kind (Neumann function) Y_0

$$\Psi_n = S_n J_0(\beta_n r) - V_n Y_0(\beta_n r), n = 1,2,3,\ldots \tag{40}$$

where the integration constants are S_n and V_n, as well as the eigenvalues β_n

are solved from the equations

$$\boldsymbol{S_n = \frac{h_3}{k_2} Y_0(\beta_n b) - \beta_n Y_1(\beta_n b)} \tag{41}$$

$$\boldsymbol{V_n = \frac{h_3}{k_2} J_0(\beta_n b) - \beta_n J_1(\beta_n b)} \tag{42}$$

$$S_n U_n - V_n W_n = 0 \tag{43}$$

where

$$\boldsymbol{U_n = \tfrac{1}{2} aK\beta_n^2 J_0(\beta_n a) - \beta_n J_1(\beta_n a)} \tag{44}$$

$$\boldsymbol{W_n = \tfrac{1}{2} aK\beta_n^2 Y_0(\beta_n a) - \beta_n Y_1(\beta_n a)} \tag{45}$$

$$K = \frac{c_1 \rho_1}{c_2 \rho_2} \tag{46}$$

Equation (34) presents a self-adjoint operator and Equations (34) - (36) are a special case of the Sturm-Liouville problem (Arfken 1985). Therefore, the eigenfunctions Ψ_n form an orthonormal set corresponding to eigenvalues β_m (m = 1,2,3,...) in the sense

$$\int_a^b r\Psi_m\Psi_n dr = \delta_{mn} N(\beta_m) \tag{47}$$

where δ_{mn} is a Kronecker delta function, and the normalisation $N(\beta_m)$ is given by

$$N(\beta_n) = \frac{2}{\pi^2} \cdot \frac{B_2 U_n^2 - B_1 V_n^2}{\beta_n^2 U_n^2} \tag{48}$$

where

$$B_1 = \beta_n^2 [1 + (aK\beta_n / 2)^2] \tag{49}$$

$$B_2 = (\frac{h_3}{k_2})^2 + \beta_n^2 \tag{50}$$

The general solution of $\vartheta(r,t)$ is now given in terms of a function series

$$\vartheta(r,t) = -T_0 \sum_{n=1}^{\infty} \frac{\exp(-\alpha_2 \beta_n^2 t)}{N(\beta_n)} \Psi_n(r) \int_a^b r' \Psi_n(r')[1/Bi + \ln(\frac{b}{r'})]dr' \tag{51}$$

3.2.6 Initial condition

The final phase to determine the complete solution given formally in Equation (51) is to carry out explicitly the integration on the left hand side over the temperature distribution given by the initial condition, Equation (31). The problem divides into two integrals, since in the brackets within the integral in Equation (51) $1/Bi + lnb$ is a constant during integration.

The second integral has an additional *lnr´* dependence. The first integral yields directly (Abramowitz and Stegun 1972)

$$\int_a^b r'\Psi_n(r')[1/Bi + \ln b]dr' =$$
$$\frac{1/Bi + \ln b}{\beta_n}\{S_n[bJ_1(\beta_n b) - aJ_1(\beta_n a)] - V_n[bY_1(\beta_n b) - aY_1(\beta_n a)]\} \tag{52}$$

The second term is solved by integration by parts

$$\int_a^b r'\Psi_n(r')\ln r'dr' = S_n\int_a^b \ln r'[r'J_0(\beta_n r')]dr' - V_n\int_a^b \ln r'[r'Y_0(\beta_n r')]dr' =$$
$$\frac{S_n}{\beta_n}\left\{/_a^b \ln r'[r'J_1(\beta_n r')] - \int_a^b J_1(\beta_n r')dr'\right\}$$
$$-\frac{V_n}{\beta_n}\left\{/_a^b \ln r'[r'Y_1(\beta_n r')] - \int_a^b Y_1(\beta_n r')dr'\right\} \tag{53}$$

which after substitutions leads to

$$\frac{S_n}{\beta_n}\left\{b\ln b \cdot J_1(\beta_n b) - a\ln a \cdot J_1(\beta_n a) + \frac{1}{\beta_n}[J_0(\beta_n b) - J_0(\beta_n a)]\right\} -$$
$$\frac{V_n}{\beta_n}\left\{b\ln b \cdot Y_1(\beta_n b) - a\ln a \cdot Y_1(\beta_n a) + \frac{1}{\beta_n}[Y_0(\beta_n b) - Y_0(\beta_n a)]\right\} \tag{54}$$

Substituting these into Equations (51) and (28), and utilising the Wronskian relationships of the Bessel functions (Gradsteyn and Ryzhik 1980) leads finally after some algebraic manipulations to the closed form solution for the temperature $T_2(r,t)$

$$\frac{T_2(r,t)}{T_0} =$$

$$1/Bi + \ln(\frac{b}{a}) - \pi \sum_{n=1}^{\infty} \frac{\beta_n U_n^2 \exp(-\alpha_2 \beta_n^2 t)}{B_2 U_n^2 - B_1 V_n^2} \left\{ 1/Bi - \frac{1}{b\beta_n} + \frac{V_n}{U_n} \left[\ln(\frac{a}{b}) - Bi + \frac{1}{a\beta_n} \right] \right\} \Psi_n(r) \quad (55)$$

3.3 CHARACTERISTIC TIME FOR HEATING

In Equation (55) the time dependence of the solution is determined by the exponentials of Equation (39), which multiply every spatial eigenfunction of the series expansion. As the characteristic nondimensional time τ we use

$$\tau = 1 / \alpha_2 \beta_1^2 \quad (56)$$

where β_1 is the smallest positive root of Equation (43). During time τ the first time-dependent term obtains 1-1/e ≈ 63% of its final value. The higher terms are then much closer to the asymptotic value, because the positive roots form a rising monotonous sequence with differences between the roots of the order 3 to 5 for the samples discussed here. Taking material values for PVC insulated copper cables of a few millimetres in diameter, we obtained values given in Table 14. The material values used are given in Table 15. The sources for the thermal data for copper are Welty et al. (1984), and for PVC insulator Gross (1985). The electric resistivity of copper is given by the cable supplier.

Table 14. Roots of the orthogonal polynomials and the shortest time constant.

Cable type	Radii (mm)		Roots					Time (s)
	a	b	$b\beta_1$	$b\beta_2$	$b\beta_3$	$b\beta_4$	$b\beta_5$	τ_1
MMAO-A	0.399	1.1	0.4944	3.725	7.964	12.675	17.507	65.7
	0.399	4.5	0.9873	3.918	6.947	10.020	13.173	276
MMAO-A	0.564	1.35	0.5386	3.853	8.589	13.795	19.105	83.4
	0.564	5	1.031	3.903	6.912	10.035	13.292	312

Table 15. Literature values of variables of cable materials.

Variable	Value copper	insulator	Dimension
Heat conductivity	379	0.16	W/Km
Density	1180	1400	kg/m^3
Specific heat capacity	1800	1500	J/kgK
Thermal diffusivity	103	0.076	mm^2/s
K	1.6		
h	20		W/Km^2
Resistivity	18.3	NA[1)]	nΩm
Biot number Bi	0.14		

[1)] NA=not applicable

3.4 HEATING OF CABLES WITH ELECTRICAL CURRENT

In these experiments, cables of type MMAO-A from a Finnish nuclear power plant were heated with electrical current in order to verify and obtain parameters for the theory presented in Section 3.2 The experiments were performed with electrical current in the range 11...83 A, as indicated by theoretical estimates presented in Figure 7. The cable was heated with constant current in each experiment until the temperature rise ceased or the conductor broke or the insulation was destroyed.

The conductors in the cables studied were polyvinyl chloride insulated and the cable was polyvinyl chloride jacketed. The number and cross-section of the stranded copper conductors in the experiments were 4 x 1.0 mm^2, 4 x 0.5 mm^2 and a single conductor of cross-section 1.0 mm^2.

The circuit diagram for the experiments is presented in Figure 4. Electric current was fed into the circuit from the battery A and monitored by measuring the voltage over the resistor R1. The current was regulated with the variable resistor R2 and the switch S. The cable Rc was 265 mm long and current was fed into one of the conductors.

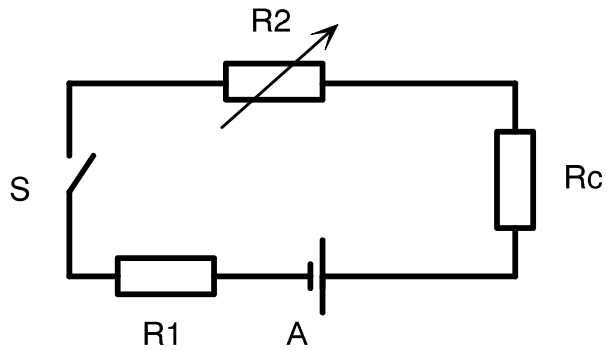

Figure 4. Circuit diagram for experiments on heating of cables with electric current. A battery, R1 resistor for current measurement, R2 current regulator, S switch and Rc cable.

Temperatures in the cable were measured with 0.25 mm K type thermocouples. Thermocouple notations and locations in different types of cable are shown in Figure 5. The thermocouples were brought into the cable through a cut about 20 mm long in the centre part of the cable jacket. The positions and notations of thermocouples are shown in Figure 5.

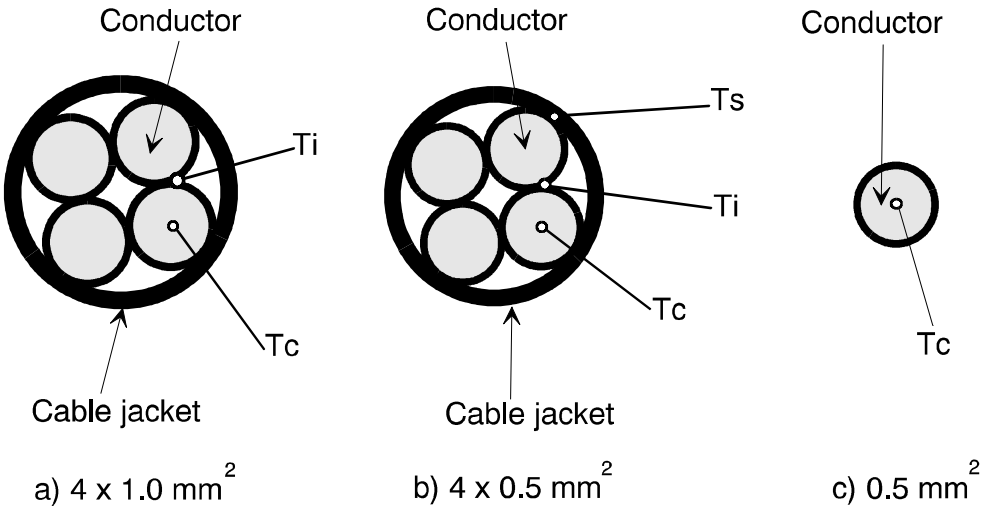

Figure 5. Schematic cross-section (not to scale) of a) and b) cable with four conductors and c) single conductor showing location of thermocouples in experiments on heating of cables with electric current. Tc thermocouple in the heated stranded conductor, Ti on the surface of the heated conductor and Ts between a non-heated conductor and the cable jacket.

The experiments with observations are listed in Table 16 and the measured temperatures are presented in Appendix 1. The cable did not burn with flame in the experiments except for a very short time in experiment 5.

3.5 COMPARISON WITH EXPERIMENTS

In Figures 6 and 7 experimental data of Figures 1 - 3 of Appendix 1 are replotted as temperature differences, and compared with predictions by theory presented in Sections 3.1 - 3.3. The experiments used were numbered 862 - 865 in Table 16 and used a cable 4x1 mm^2. The upper curves (diamonds) in Figure 6 present temperatures of the conductor insulation, and the lower curves (circles) the temperature of a copper wire of the cable. Theoretical curves were fitted by using a calculated time constant τ_1 from Table 14, and adjusting temperature change amplitude to fit the data. This worked so well for the temporal development of temperature rise that most theoretical curves are hidden invisibly behind the experimental data points. Only the first term in the sum of Equation (55) was used.

In Figure 7 the measured temperature differences are plotted as dots, and compared with theoretical data of the steady state solution predicted using Equation (26). It can be seen the agreement is rather good despite a fair difference in the geometry of the cable used (Figure 5a) as compared with the model used for theory (Figure 3).

Table 16. Experiments on heating of PVC insulated and PVC jacketed cables with electrical current. Ae = after the experiment. Sample = new denotes cable not heated before and sample = previous denotes cable used in the previous experiment.

No	Code	Cable type, sample	Current (A)	Course of experiment Time (min:s)	Observation
1	862	4 x 1.0 mm^2, new	11	0:00	Current on
				5:05	Current off
				Ae	No external damage was observed
2	863	4 x 1.0 mm^2 previous	22	0:00	Current on
				8:00	Current off
				Ae	No external damage was observed
3	864	4 x 1.0 mm^2 previous	42	0:00	Current on
				13:00	Current off
				Ae	No external damage was observed
4	865	4 x 1.0 mm^2 previous	59	0:00	Current on
				1:12	First smoke from the upper end of the cable
				5:30	The conductor feeding current broke above the cable
				Ae	No external damage was observed on the jacket
					The cut in the jacket for the thermocouples was widened about 1 mm
5	866	4 x 1.0 mm^2 previous	83	0:00	Current on
				0:54	A small flame from the upper end of the cable
				1:04	The flame went out
					Smoke from the upper end of the cable and from the cut in the jacket
				1:45	The current feeding conductor broke above the cable
				Ae	The upper part of the jacket was partly melted and deformed
					About 75% of the length of the insulation of the current feeding conductor was charred
6	867	4 x 0.5 mm^2, new	11	0:00	Current on
				7:02	Current off
				Ae	No external damage was observed
7	868	4 x 0.5 mm^2 previous	20	0:00	Current on
				12:02	Current off
				Ae	No external damage was observed
8	869	4 x 0.5 mm^2 previous	38	0:00	Current on
					Smoke from the cable during the experiment
				13.20	Current off
				Ae	No external damage was observed
					Considerable instability of Tc was noticed during the experiment indicating loose contact with the conductor

To be continued on the next page

Continued from the previous page

No	Code	Cable type, sample	Current (A)	Course of experiment Time (min:s)	Observation
9	870	4 x 0.5 mm^2 previous	52	0:00	Current on
				0:20	Smoke from the cable
				2:30	The jacket is melting
				3:30	Much smoke
				5:30	The current feeding conductor broke above the cable
				Ae	The jacket was partially melted and deformed all over its surface and the conductors are exposed at some places The insulation of all four conductors in the cable was charred
10	871	4 x 0.5 mm^2 previous	51	0:00	Current on
				0:20	Smoke from the cable
				3:10	The surface of the jacket is bubbling
				3:45	The conductors are exposed in some parts of the jacket
				7:00	The smoke is decreasing
				7:50	The current feeding conductor broke above the cable
				Ae	About 50% of the jacket was consumed The insulation of all four conductors was charred and partially consumed
11	872	1 x 0.5 mm^2, new	21	0:00	Current on
				5:00	Current off
				Ae	No external damage was observed
12	873	1 x 0.5 mm^2 previous	38	0:00	Current on
				0:51	Smoke
				0:57	Tc comes out from the conductor when the insulation melts
				1:04	The insulation is bubbling
				5:20	Current off
				Ae	The insulation of the conductor was charred and partially consumed
13	874	1 x 0.5 mm^2 new	36	0:00	Current on
				0:50	Tc comes out from the conductor when the insulation melts
				1:02	The insulation is bubbling
				5:00	Current off
				Ae	The insulation of the conductor was charred and partially consumed

From Figures 4 - 13 in Appendix 1, great deviations from the smooth curves of Figure 6a are observed. There are at least two reasons for these deviations:

(1) High DC heating current strongly disturbed temperature measurements by thermocouples as shown very clearly in Figures 6 and 7, less clearly in Figures 8 and 9 of Appendix 1. Symmetric deviation of thermocouples (Ts and Tc) from the indication of (Ti) show electromagnetic interference with thermocouples connected to the data acquisition system.

(2) Physico-chemical effects connected with evaporation and boiling of cable insulation materials leading to phenomena and boundary conditions are not at all considered in the theory presented here. It is shown most clearly in Figures 12 and 13 of Appendix 1.

It is not surprising electromagnetic interference disappears as the heating current is switched off, but also all other types of sudden changes disappear as witnessed by very smooth temperature decay curves in Figures 1 - 13 of Appendix 1.

It can be concluded from the tests that we can use simple theoretical predictions (Equation (26) to calculate maximum temperature rise for a cable heated from overcurrent. The time scale of the heating phenomenon is predicted by a time constant obtained from Equation (56) calculated by using the smallest positive root of Equation (43). Finally, temporal behaviour of heating is well predicted for similar cables as used here by Equation (55), where only the first term in the series contributes significantly.

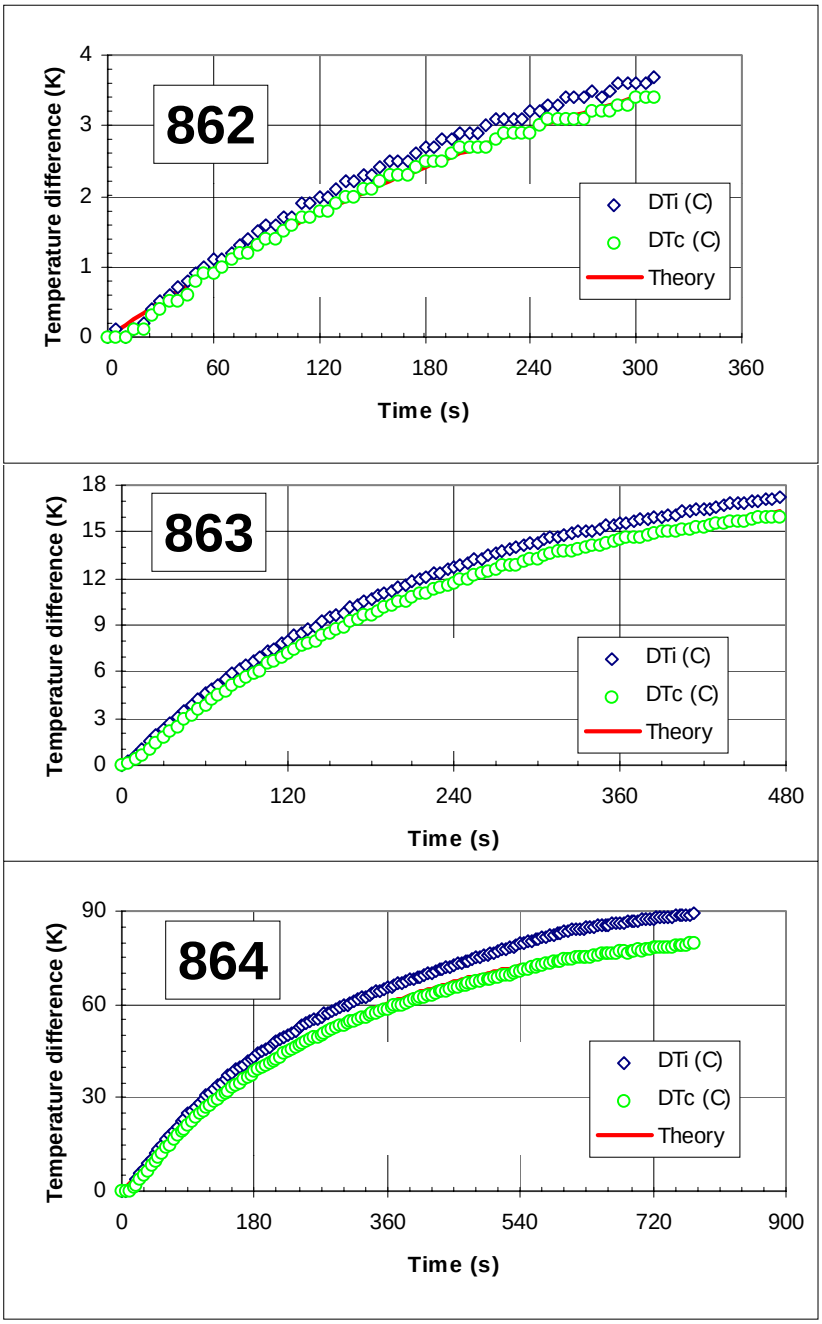

Figure 6. Heating of cables from overcurrent. Theoretical lines are hidden behind the lower curve (DTc (C)) so well, that the full line is not visible.

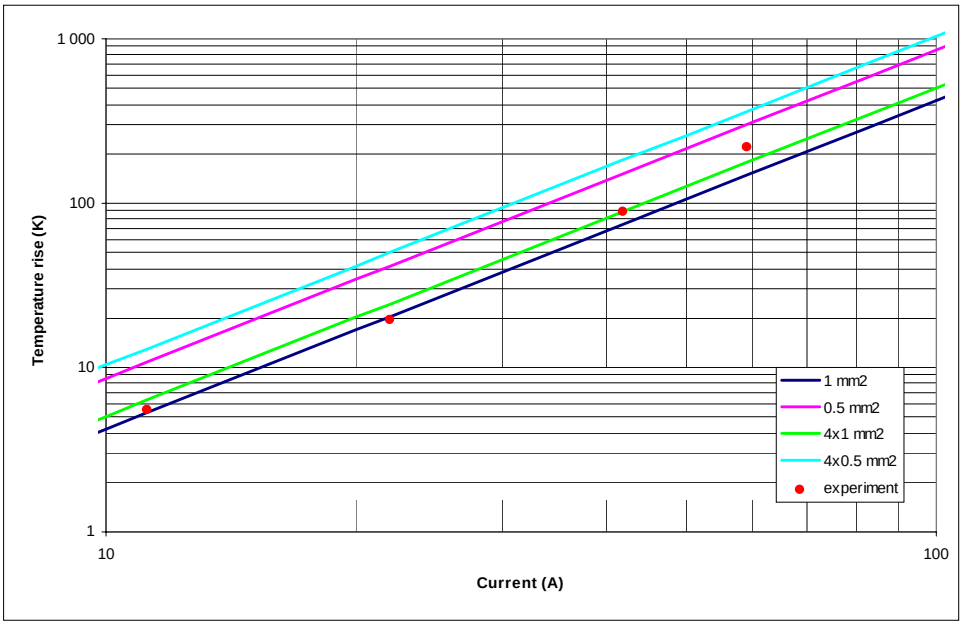

Figure 7. Heating of cables from overcurrent. Full lines are theoretically calculated maximum temperatures for different types of cables, and the dots experimentally measured data from tests 862 - 865 using a 4x1 mm^2 cable.

4 SELF-IGNITION OF A REACTING CABLE

A cable with a plastic insulator is a system capable of self ignition if the electric current in the conductor produces more heat than is carried out through the outer surface of the cable. The self-heating problem has been treated in several textbooks (Bowes 1984, Lees 1980), and in many special articles (Thomas and Bowes 1961, Bowes and Langford 1968, Bowes 1974, Gray et al. 1990). Since the details in several treatises differ slightly from the goals pursued here, we reiterate the salient features of the theory.

4.1 THEORY OF SELF IGNITION OF A CABLE

In a self-heating material a chemical reaction produces heat, which could either be stored in the material or escape the system through boundaries. If the amount of heat produced exceeds the amount transferred from the system, a thermal explosion, an uncontrolled increase of system temperature, might follow. This is the mechanism of self-heating often leading to self-ignition. A cable or a bundle of cables is in principle a potentially self-igniting system although cable insulation is not a typical self-igniting material. When a cable is thermally insulated, as in a penetration, and simultaneously carries a current, self-ignition is possible if the design values of the system are exceeded for some reason. A cable or a bundle of cables can be modelled for heat transfer as a cylindrical object depicted in Figure 8 reducing mathematically to a one-dimensional system. It is assumed for simplicity there is a single metal core of radius r_i surrounded by an electrical insulation material of radius r_s. In a steady state the inner surface of the insulation is at temperature T_i and the outer surface at temperature T_s. In a long cable, temperature varies only in the direction of radius r.

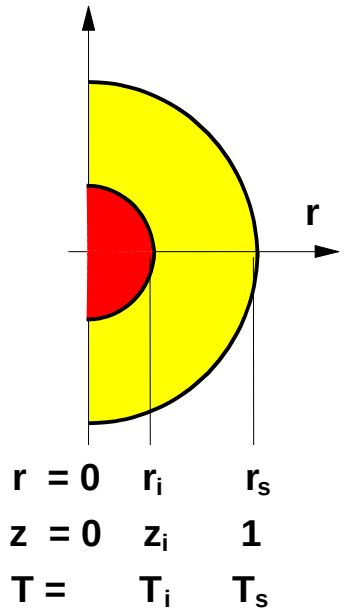

Figure 8. Notation of co-ordinate axes, and temperatures of boundary conditions of an asymmetrically heated cylindrical object.

For a self-heating heat balance equation assuming zero order kinetics, chemical reactions can be cast in the form (Thomas 1958, Lees 1980)

$$\frac{d^2\theta}{dz^2} + \frac{1}{z}\frac{d\theta}{dz} = -\delta \exp(\theta) \tag{57}$$

where non-dimensional temperature θ, and radius z are given by

$$\theta = \frac{E}{RT_s^2}(T - T_s); \quad \theta > 0 \tag{58}$$

$$z = \frac{r}{r_s} \tag{59}$$

Criticality parameter δ will be defined later. The general solution of Equation (58) is of the form (Chambré 1952)

$$\theta = \ln\left(\frac{2F^2 G z^{F-2}}{\delta(1+Gz^F)^2}\right) \tag{60}$$

where the integration constants F and G are determined from boundary conditions

$$\theta = 0; z = z_i \tag{61}$$

$$\theta = \theta_s; z = 1 \tag{62}$$

Adding a practical criticality condition on the inner surface

$$\frac{d\theta}{dz} = 0; \quad z = z_i \tag{63}$$

leads finally to calculation formulas for the constants *F* and *G* as well as the criticality parameter δ_c

$$G = \frac{F-2}{F+2} z_i^{-F} \tag{64}$$

$$\exp(\theta_s) = \frac{(1+Gz_i^F)^2}{(1+G)^2} z_i^{-F+2} \tag{65}$$

$$\delta_c = \frac{2F^2 G}{(1+G)^2} \exp(-\theta_s) \tag{66}$$

Nonlinear Equations (64) - (66) are solved numerically by iteration.

4.2 SELF-IGNITION EXPERIMENTS

Self-ignition temperatures for a single cable and a bundle of cables were determined with method NT FIRE 045 (Björkman and Keski-Rahkonen 1992). The cable was of the same type as described in Section 3.4, with polyvinyl chloride insulated conductors and cable jacket, number and cross-section of conductors 4 x 1.0 mm^2. The bundles consisted of 7 and 19 cables and they were tied together with steel wire. The cable or cable bundle was on a bed of mineral wool with its ends insulated with a 25...30 mm thick layer of mineral wool during the test as shown for single cable

in Figure 9. The length of the exposed part of the sample was 190 mm in experiment 1 and 200 mm in experiments 2 and 3.

Temperatures were measured with 0.25 mm K type thermocouples located at the centre of the bundle Tc, halfway from the centre outwards Th and on the surface of the bundle Ts. Longitudinally the thermocouples were located in the middle of the cable (Figure 9). Thermocouple Tc was drawn into the cable from its end with one of the conductors without damaging the cable surface. Thermocouples Th and Ts were tied to the cables so the end of the thermocouple was in contact with the cable surface. Cross-sections of the samples and thermocouple locations are shown in Figure 10.

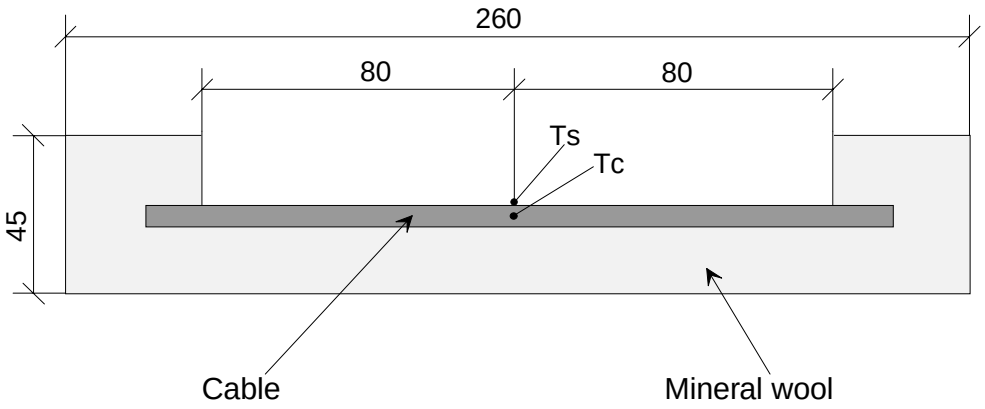

Figure 9. Side view of single cable with mineral wool insulation. Tc thermocouple at centre of cable and Ts at the outer surface. Dimensions in mm.

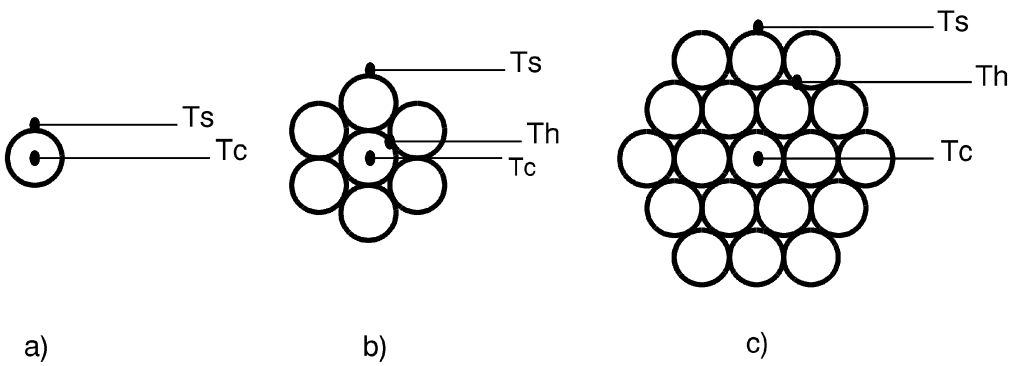

Figure 10. Cross-sections of cable bundles and thermocouple locations in self-ignition experiments. a) single cable, b) bundle with 7 cables and c) bundle with 19 cables. Tc thermocouple at centre of cable in centre of bundle, Th at halfway point of bundle and Ts on the outer surface of the outermost cable.

The experimental parameters and the main results are presented in Table 17. Original temperature curves and curves where the furnace temperature is subtracted from the cable temperatures are presented in Appendix 2. Ignition temperatures were determined graphically from the temperature difference curves according to the following procedure (Björkman and Keski-Rahkonen 1992): a straight line is drawn as the continuation of the linear temperature rise of the sample during the regular regime and another as a tangent to the inflection point of the heating part of the curve. The ignition temperature and corresponding time are then determined at the crossing point of these lines. The method is demonstrated in Figure 1b of Appendix 2.

If the temperature difference curves showed two distinct rises, two temperatures T1 and T2 were determined.

The cable jacket was consumed after the tests, pieces of it were under and around the bundle and between the cables. The Al-foil around the conductors was mostly intact, still surrounding the conductors, some foils had longitudinal gaps. The insulation around the conductors was charred.

Table 17. Results from self-ignition experiments on PVC-insulated and PVC-jacketed 4 x 1.0 mm^2 cable and cable bundles.

Experiment no		**1**		**2**		**3**	
Number of cables		1		7		19	
Sample radius (mm)		5		15		25	
Heating rate (mK/s)		1.7		5.6		5.6	
Initial/Final sample mass (g/g)		35.0/16.2		242.4/132.0		648.7/349.4	
Mass loss (%)		54		45		46	
Ignition temperatures T and corresponding times t		T (°C)	t (min)	T (°C)	t (min)	T (°C)	t (min)
Centre:	T1	228	2100	271	757		
	T2	289	2700	360	886	288	674
Halfway:	T1	-	-	263	735		
	T2	-	-	343	888	303	683
Surface:	T1	298	2830	224	629		
	T2	370	3555	316	886	306	692

4.3 CONCLUSIONS

Using data in Table 17, material parameters presented in 4.1 could have been determined. The temperatures observed were, however, so high, that this determination would be of only academic interest. Therefore, it was not carried out here. In conclusion, it could be said that although self ignition of a PVC cable bundle is in principle possible, the temperatures are so high that it is rather improbable the phenomenon would lead to a primary cause of a fire.

5 IGNITION OF A CABLE FROM A SHORT CIRCUIT

A short circuited cable creates an arc between the corresponding wires. The arc creates high temperatures and produces intensive heat in a small volume. It also melts the wire and therefore travels some distance along the cable during arcing.

5.1 PHYSICAL PRINCIPLES OF AN ELECTRIC ARC

A man-made, long lasting electric arc has been known for more than two hundred years. Thermal buoyancy bends a long discharge column upwards giving the name arc to the phenomenon, the equivalent of which is used in several languages. Some thorough articles give general overviews of the physics and experiments in the arc (Hagenbach 1927, Maxfield and Benedict 1941, Meek and Craggs 1953, and Finkelnburg and Maecker 1956). Kohn and Guckel (1924) have measured electrical characteristics of arcs of carbon electrodes in different atmospheres. Finkelnburg (1948) published a whole monograph on carbon arcs, and Weizel and Rompe (1949) a monograph on the theory on electrical arcs and sparks. Since then very little research reported in open literature has been done on arcs, although research on other areas of plasma physics has been developed very intensively (Kunkel 1966). Below, a number of equations and phenomena are reviewed to allow a general physical explanation of the major components of arcs.

The current in a plasma arc is carried mainly by electrons. Different cathode materials are able to emit various current densities *I"* because of different material properties. The Dushman-Richardson equation gives for the current density I'' on the cathode of the arc gap (Dekker 1964)

$$I'' = AT^2 e^{-\phi/kT} \tag{67}$$

where a constant A = 1.2 μA/m^{2}K^2, Boltzmann constant k = 86.17 μeV/K, ϕ is work function [eV], and T absolute temperature. Calculating for materials found in electronic cabinets, maximum values of current densities at the melting ($\boldsymbol{T_m}$) and evaporation (sublimation) ($\boldsymbol{T_e}$) temperatures are given in Table 18.

Table 18. Physical parameters of materials which in principle would contribute to thermionic electronic emission.

Material	**ϕ [1] (eV)**	**T_m [2] (K)**	**T_e [2] (K)**	**I''_m (A/m^2)**	**I''_e (A/m^2)**
Carbon	5.0	3820	3640	$4.4 \cdot 10^{6}$	$1.9 \cdot 10^{6}$
Copper	4.65	1356	2840	$1.1 \cdot 10^{-5}$	$5.4 \cdot 10^{4}$
Gold	5.1	1337	3353	$1.2 \cdot 10^{-7}$	$2.9 \cdot 10^{5}$
Iron	4.5	1808	3023	1.1	$3.4 \cdot 10^{5}$
Tin	4.42	505	2543	$2.4 \cdot 10^{-33}$	$1.3 \cdot 10^{4}$
Tungsten	4.54	3683	5933	$1.0 \cdot 10^{7}$	$5.9 \cdot 10^{9}$

1. Reference (CRC 1984, p. E-76).
2. Reference (CRC 1984, p. B-7 - B-43).

From these calculations one sees clearly that only for carbon and tungsten can current densities observed in arcs be explained using thermionic electronic emission from the cathode. Weizel and Rompe (1949) have explained cold cathode emission, which agrees with observations. In this theory the material of the electrodes plays only a secondary role. The arc is divided into zones depicted in Figure 11.

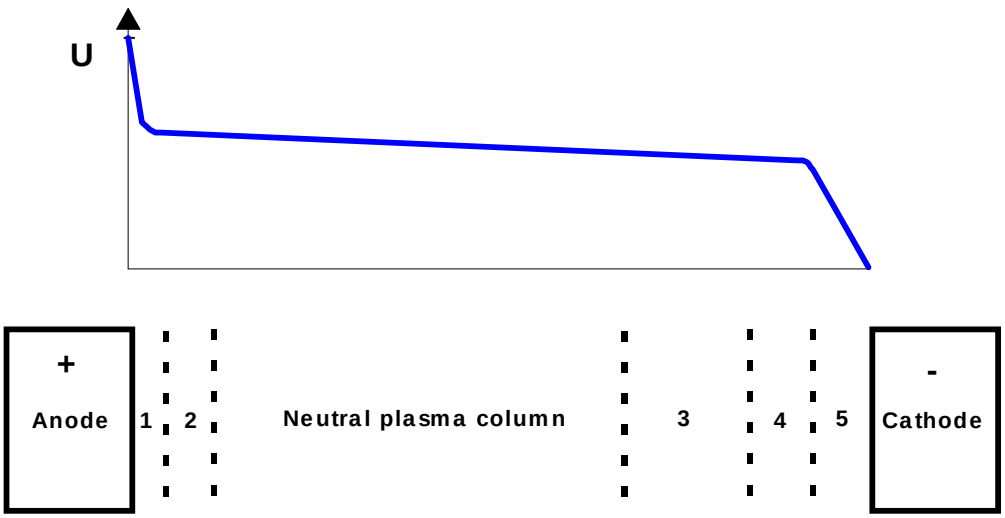

Figure 11. Different zones of conduction (lower part), and potential distribution (upper part) between electrodes in electric arcs explained in detail in text (not to scale), (Weitzel and Rompe 1949, Finkelnburg and Maeckel 1956).

The main part of the arc is occupied by the neutral plasma column, where ionised high temperature plasma (up to 10 000 K) carries electricity. Electrons carry most of the current because of high mobility although the number densities of electrons and ions are the same. The flow of current in the column is resistive. In Figure 12 the strength of the electric field is given as a function of the total current (Finkelnburg and Maecker 1956). The plasma column attaches to the anode and cathode through thin layers of other zones (Figure 11), which is vital to explain the physical phenomena observed.

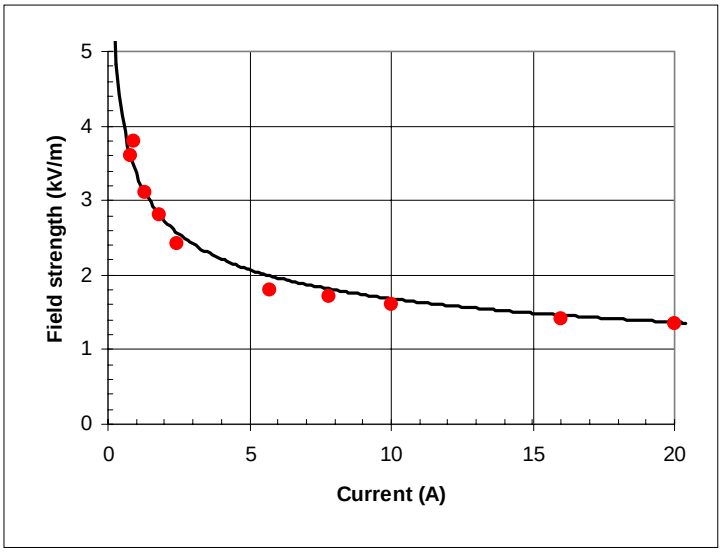

Figure 12. Strength of the electric field inside plasma column in an arc through 101 kPa pressure nitrogen, (Finkelnburg and Maecker 1956).

On the anode accelerated electrons hit it creating a negative space charge zone (1) close to the surface. The space charge causes the anode fall of the accelerating voltage. From greater a distance, up to the limit of heat conduction zone (2) and the plasma column, the hot plasma is cooled conductively by the cold anode.

On the cathode a similar cooling zone (3) from unperturbed plasma up to the surface of the cathode is formed. The temperature of the plasma drops sharply and its conductivity decreases rapidly when approaching the cathode surface. In heat conduction zone (3) despite the temperature drop, the plasma is similar to that in the column. The potential difference over

this zone is some volts. In the ionisation zone (4) gas atoms are heavily ionised creating an electron current towards the column, and an ion current towards the cathode. The potential difference is less than the ionising potential of the gas (air atoms about 14 eV, smaller for molecular species). Finally, a positive space charge zone (5) is responsible for most of the potential fall at the cathode. A detailed model by Weizel and Rompe (1949) is able to explain the current flow and forming of focuses even in the extreme case, where the whole of the electric current is carried on the cathode by ions (cold cathode). This model also explains why current flows equally well for an ac current source. A hot cathode source would be rectifying.

This results in the conclusion that the material of the electrodes plays a minor role in the physics of the arc discharge. Materials influence the heat transfer close to electrodes, the constitution of the ions in the plasma, and its radiation properties. When the arc current becomes big enough, evaporation from the cathode becomes a destabilising factor for the arc causing it to ‘hiss’. A hissing arc extinguishes because of unstable current flow. A cable insulation evaporates faster than electrode materials. Therefore, the hissing phenomenon occurs much more easily.

In Figure 13 the flow lines for a 200 A arc are given on the left hand side and contours of equal velocity (m/s) on the right hand side. In Figure 14 the isotherms (in K) in the arc are given for a 200 A discharge.

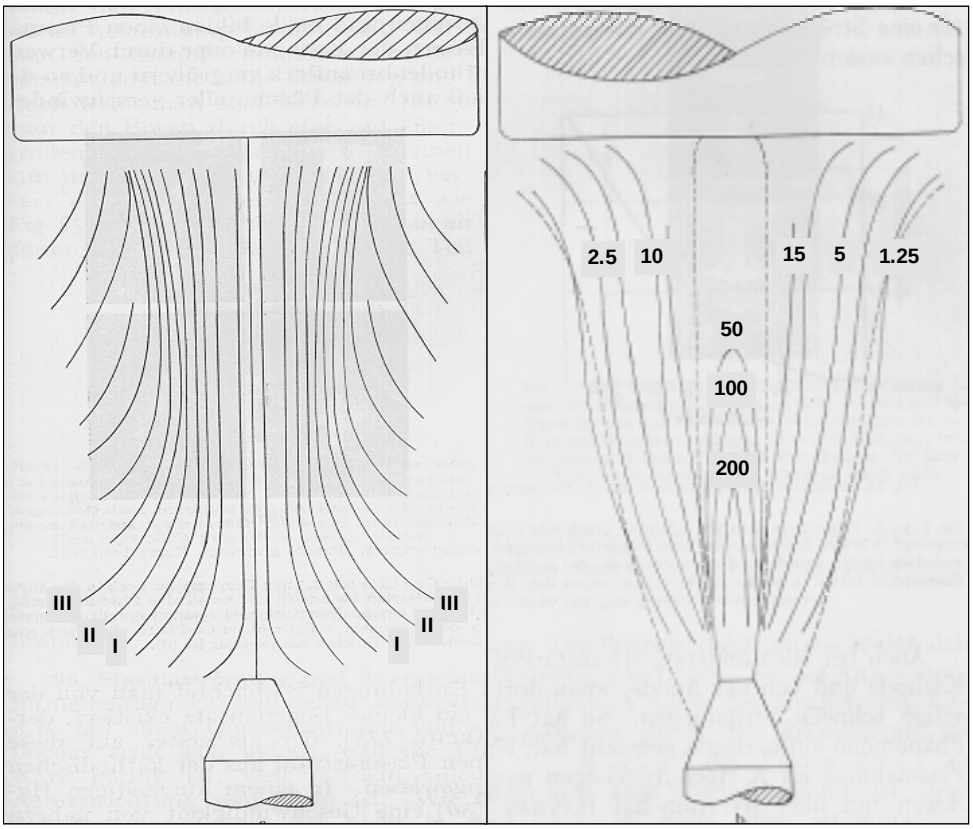

Figure 13. Flow lines (left) and contours of equal velocity (m/s) (right) in an arc of 200 A, (Finkelnburg and Maecker 1956).

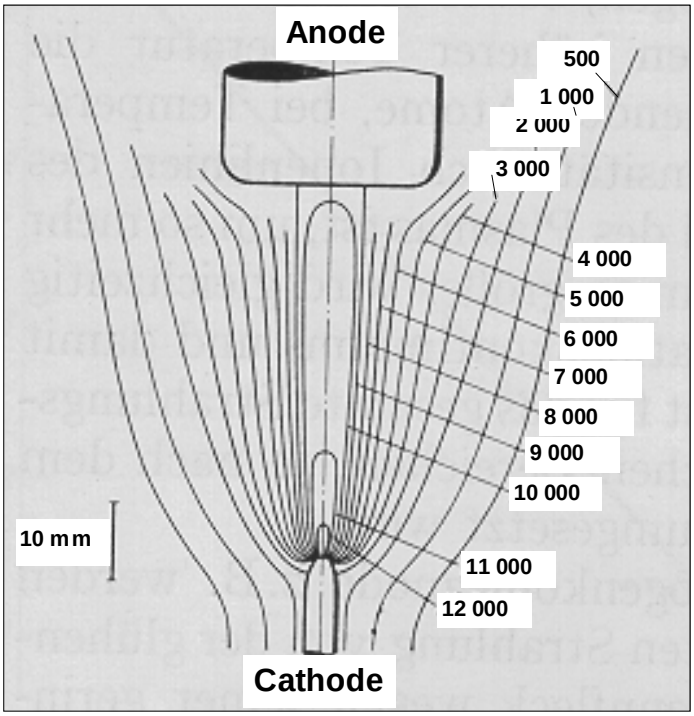

Figure 14. Isotherms (in K) of an arc of 200 A, (Finkelnburg and Maecker 1956).

Quantitative experiments carried out a hundred years ago by Mrs Hertha Ayrton (1895) give a practical formula to relate the length *l* of the arc with electrical voltage difference *U* and current *I*

$$U = \alpha + \beta l + \frac{\gamma + \delta l}{I} \tag{68}$$

where α, β, γ and δ are constants depending on the material of the electrodes. Table 19 gives values of these constants for carbon, copper and iron. These data are configuration dependent but give good guidance for technical dimensioning of the arc. In Figure 15 the voltage of the arc is plotted as a function of current for some gap widths of copper electrodes, and indicate some loading lines with given output resistance.

Table 19. Coefficients of Ayrton's equation for some materials (Hagenbach 1927).

Metal	α (V)	β (V/m)	γ (W)	δ (W/m)
Carbon	45.75	3.33	35.7	19.31
Copper	26.61	2.22	32.49	18.65
Iron	15.01	9.44	15.73	2.52

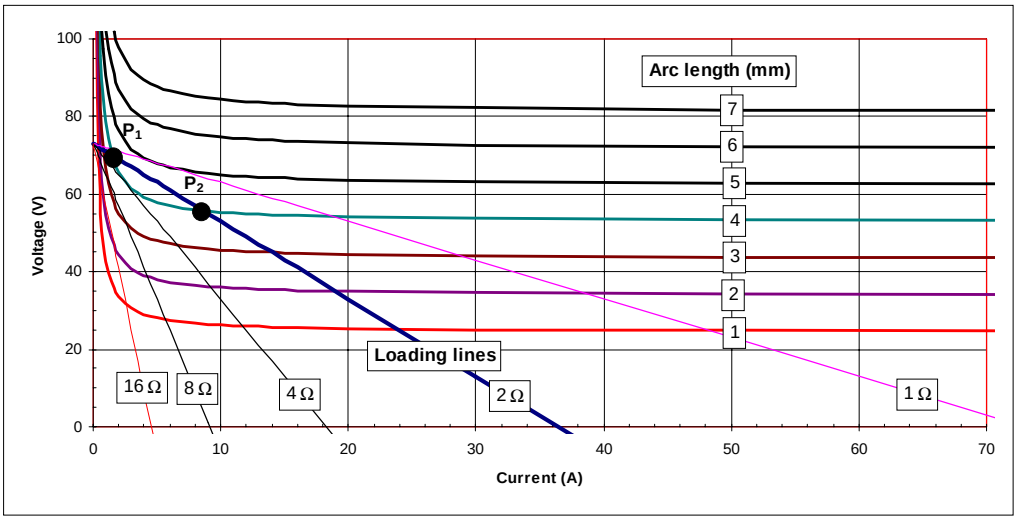

Figure 15. The voltage of an electric discharge over copper electrode arc gap as a function of current. Crossing points with loading line indicate operating points, where only P_2 is stable (Finkelnburg and Maecker 1956) .

The energy of the arc is supplied by a circuit described in principle in Figure 4. Since the load outside the arc is mainly resistive, the stable points of the arc are determined by plotting a loading line on Figure 15. For zero current the voltage is the battery voltage E, and for zero voltage the current is a short circuit current

$$I_s = \frac{E}{R_s + R} \tag{69}$$

where R_s is the inner resistance of the battery and R is the resistance of the outside load (within the arc).

The operating points of the arc are determined by the points where the arc characteristics cross the loading line. The low current cutting point P_1 is not stable, and therefore the currents increase to the higher value P_2.

The voltage U_2, and current I_2 of point P_2 are given in terms of Ayrton parameters by

$$U_2 = \tfrac{1}{2}\left(E + \alpha + \beta l - \sqrt{(E - \alpha - \beta l)^2 - 4R(\gamma + \delta l)}\right) \tag{70}$$

$$I_2 = \frac{1}{2R}\left(E - \alpha - \beta l + \sqrt{(E - \alpha - \beta l)^2 - 4R(\gamma + \delta l)}\right) \tag{71}$$

The maximum value of the spark gap for a pair of electrodes and a power source is obtained at the point where the two points P_1 ,and P_2 merge, i.e. the loading line becomes a tangent to the voltage-current characteristics of the arc. In Table 20 some values of the maximum spark lengths for copper electrodes are given as a function of the voltage and resistance of the power source as calculated from Ayrton's Equation (68). The maximum output resistance of the power source is given at this operating point by

$$R_{\max} = \frac{(E - \alpha - \beta l)^2}{4(\gamma + \delta l)} \tag{72}$$

Table 20. S*ome values of the maximum spark lengths (mm) for copper electrodes are given as a function of the voltage and 2 Ω output resistance of the power source as calculated from Ayrton's Equation (68).*

Anode voltage (V)	**Carbon**	**Copper**	**Iron**
24	-	-	0.6
36	-	2.9	1.8
48	-	6.1	3.0
73	5.9	15	5.8

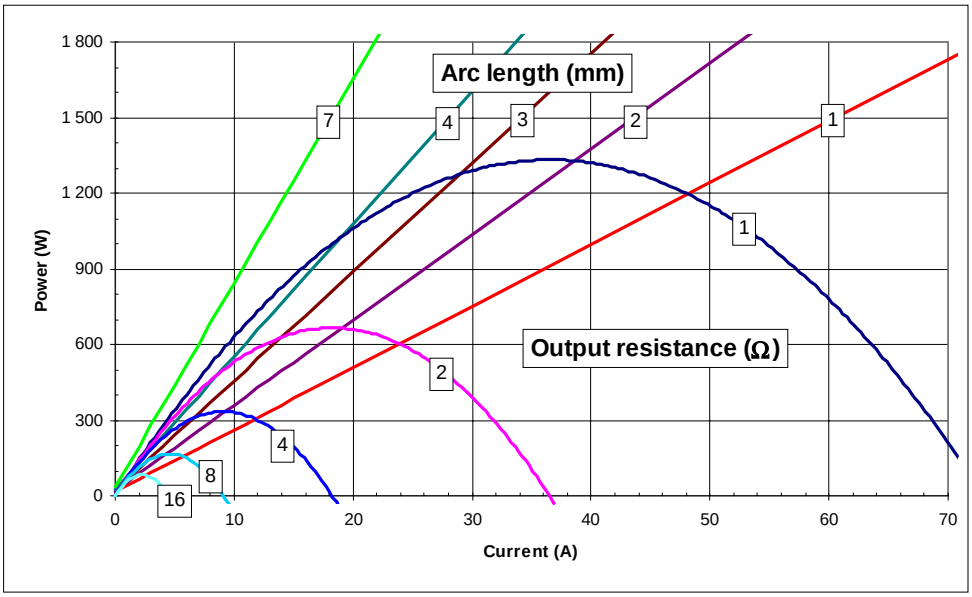

Figure 16. The power dissipated by an electric discharge over copper electrode arc gap as a function of current for different output resistance of the energy source.

In Figure 16 the power dissipated by an electric discharge over copper electrode arc gap is plotted as a function of current. The stable operating point (P_2 of Figure 15) of an arc of a given length is the crossing point of the arc length line, and output resistance parabola. For example for a 2 Ω resistance and 1 mm spark gap, the power is 600 W. One sees arcs produce heat intensively in a small volume and act as point source ignitors. However, the amount of heat produced might be so great, that a flame is blown off, and no sustained ignition is obtained. This might happen for example in a faulty cable, where the first ignited fuel is the cable insulation. If the output resistance of the power source increases, the dissipated power reduces so much that favourable conditions for ignition are created.

5.2 SHORT CIRCUIT EXPERIMENTS OF CABLE IGNITIONS

Several series of experiments to ignite a cable in different configurations and using different electrical inputs for the arc were carried out. Cable burned, but the process was so unstable it was practically impossible to create an arc lasting for more than 10 s. The experiments required high currents, which for the project were only available using commercial welding machines. They neither allowed control of the outer electrical conditions for the arc, nor quantitative measurement of the electrical parameters needed.

The reason for difficulties is believed to lie, in addition to some haphazard test methods, in the easy, and fast melting process of copper wire, vibration of cable due to electromagnetic forces created by arc plasma flow, and flow of melting plastic and pyrolysis fumes. These are all factors which during technical welding are avoided using either a coated welding rod or argon as protective inert gas around a tungsten electrode. Also, eyewitness experience was that the arcs created were so strong, they blew out the flame, because of a lack of electrical control of the discharging circuit. It was noticed later, as will become apparent from material in Chapter 7, that the release of power was possibly much too fast and violent to lead to accelerating flame.

As a summary, ignition of cables or flammable material inside an electronic cabinet is possible from a short circuit. The governing parameters describing ignition are the rate and the amount of heat released during arcing. Arc ignitions are electrically very fast phenomena. The characteristic time leading to ignition is, therefore, determined by the time constant of flame spread.

6 IGNITION OF A CABLE FROM A GROUND FAULT

In a ground fault an electric arc is created which in principle differs only marginally from the short circuit arc. In an electronic cabinet the ground is most often connected to the body of the cabinet. In the ground arc a major part of the energy is conveyed to the grounded body. If it is a thin steel plate it heats up quickly, and can result in ignition in a way similar to a short circuit.

Some tests on overheated components other than cables were carried out as described in Chapter 8. If a component is on a printed circuit or any other material of poor heat conduction, local heating is created. This led to ignition in some of the cases tested.

Explosive releases of large amounts of electrical energy are not treated theoretically or experimentally in this paper.

7 SPREAD OF FLAME ON CABLES

7.1 THEORY OF FLAME SPREAD ON CABLES

No specific, generally accepted theory of flame spread on cables exists. The whole flame spread theory on solid material is not yet well established although many approaches have been proposed. The most practical concurrent flame spread model proposal has been by Saito et al. (1986) and a related proposal by Hasemi (1986). These models are very practical although theoreticians consider them fairly rude. Delichatsios and Delichatsios (1994) proposed a theory of flame spread on PVC cable, which used rather similar approaches to ours but made use of the special calorimeter available only at Factory Mutual Research. The goal was to be able to simulate a cable test experiment on a 914 mm high cable tray using 100 x 100 mm^2 cable samples. Recently Quintiere and Lee (1998) have published studies on the effect of ignitor on flame spread, which gave similar results to those we obtained here.

The model adopted here is the one presented by Saito et al. (1986). In its simplest form it allows for analytical solutions for simplified material properties (Thomas & Karlsson 1990, Baroudi & Kokkala 1992). For designing these experiments, results of a paper by Hasemi at al. (1994) were utilised.

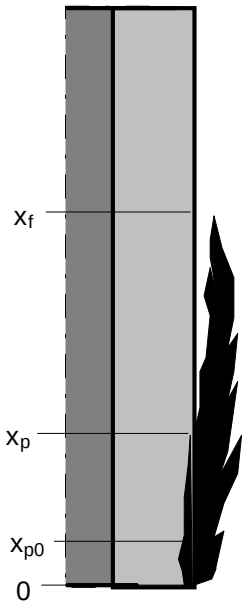

Figure 17. Model of flame spread on cable insulation (light grey) on a metal core (hatched). x_{p0} is the length of the pilot flame, x_p length of pyrolyzing zone, and x_f length of the flame (adapted from Saito et al. 1986).

When applying the model to cables drafted schematically in Figure 17, we ignore first the cylindrical geometry, and second (more important) the presence of the central metal wire. The velocity of the pyrolysing front $v_p(t)$ is given by a Volterra type of integral equation

$$v_p(t) = (x_f - x_p)/\tau = (KQ_l + x_b - x_p)/\tau =$$
$$\frac{1}{\tau}\left\langle \begin{array}{l} K\left\{Q_0(t)\left[U(t) - U(t-t_b)\right] + x_{p0}q(t) + \int_0^t q(t-\xi)v_p(\xi)d\xi\right\} + \\ \left[\int_0^{t-t_b} v_p(\xi)d\xi + x_{p0}\right]U(t-t_b) + \left[x_{p0} + \int_0^t v_p(\xi)d\xi\right] \end{array}\right\rangle \quad (73)$$

where $Q_0(t)$ is the heat release rate of the pilot ignition source, x_b the length of burnoff front, x_{p0} the length of pilot flame and $q(t)$ local heat release rate per unit area. The length of pyrolysing zone is x_p, the length of flame x_f, heat release per unit width of pilot Q_0, and burning

insulation Q_l. K is an experimental constant and τ a characteristic time for ignition of the material.

Assuming heat release $q(t)$ from a thin layer of cable insulation fuel at a given location is a constant q_0 until burnoff t_b, the heat release is given mathematically by

$$q(t) = q_0 \left[U(t) - U(t - t_b) \right] \tag{74}$$

where $U(t)$ is Heaviside's unit step function. For sustained pilot flame of constant rate Q_0 the Laplace transform of Equation of (73) yields (after rearranging of terms)

$$\frac{v_p(s)}{x_{p0}} = \frac{(Q_0 / x_{p0} - s + Kq_0)\left[1 - \exp(-t_b s)\right]}{\tau s + (1 - Kq_0)\left[1 - \exp(-t_b s)\right]} \tag{75}$$

Direct inversion of Equation (75) is rather complicated, and a closed form solution is not known. Inspecting the asymptotic behaviour of velocity $v_p(t)$ ($t \to \infty$, which in s-space is equivalent to $s \to 0$) from the inverse transformation of Equation (75), it is noticed that to the lowest order of s it will be a sum of exponentials. The temporal behaviour of the velocity is determined by the sign of the real roots of the denominator of Equation (75): they will lead either to deceleration or acceleration. The criterion line becomes very simple

$$\frac{\tau}{t_b} \quad \begin{cases} > & a - 1 \quad \textit{decelerates} \\ < & a - 1 \quad \textit{accelerates} \end{cases} \tag{76}$$

where $a = K_{q0}$.

This is presented graphically on a $\tau - a$ -plane in Figure 18. Acceleration of speed continues according to this model for as long a distance as there is material available. In the depth direction, burning continues until burnoff (LB local burnoff). This happens, when the points fall below the heavy line. Deceleration happens gradually. In Figure 18 there are three additional lines plotted showing the distance of flame front extinguishing x_{poff} scaled with pilot flame height. For a decelerating flame from a

sustained pilot flame, the flame front proceeds to some distance, and then extinguishes by itself (LS local spread). If extinguishing happens essentially at the distance of pilot flame length itself, it is called local ignition (LI).

Which category the burning vertical material item falls into, depends essentially on two nondimensional parameters, the ratio of ignition time τ to the burnoff time t_b and the heat release rate q_0 made nondimensional by multiplying an experimental constant K.

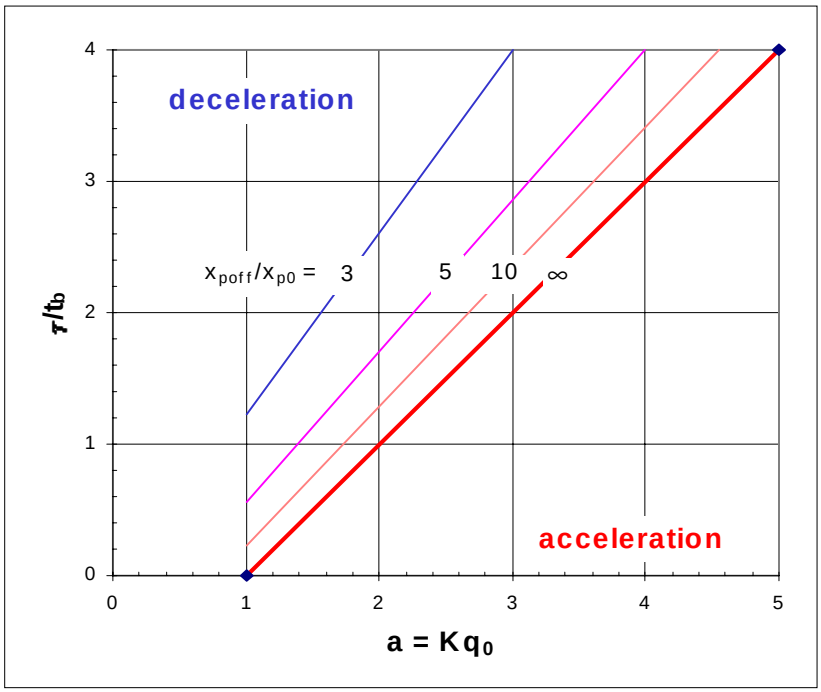

Figure 18. Critical conditions of flame spread on vertical solid material (Hasemi et al. 1994).

The validation of this model for cable applications is not very well established yet because of thin insulation layers and a heavy metal core with a considerable heat capacity. Therefore, no quantitative application was attempted. Qualitatively, it is believed even for cables three modes of burning, LB, LS, and LI, are valid. For classification of cables it would be very important to know to which category a cable belongs, but so far this methodology has not yet established itself.

7.2 FLAME SPREAD EXPERIMENTS ON CABLES

Small energy release from a burning cable is usually not sufficient to cause total burnout of a container, such as an instrument cabinet, where the cable is located. Since according to statistics presented in Section 2 cables are probable ignition sources, small-scale experiments were carried out for some classes of common cables used in NPPs to validate qualitatively the predictions of the above theory, and to find under what ignition conditions sustained burning is possible. In addition to the simple half space geometry shown in Figure 17, a space configuration of the burning cable also became relevant.

For reproducibility of tests, gas flame ignition was used. The burner was a 100 mm wide tube with holes 1 mm in diameter every 10 mm. At the relevant range or power, it produced a stable planar flame, the length of which could be controlled by adjusting gas flow. A short series of tests was carried out. In Figure 19 the first test using KJPP wiring was made by igniting it using a match. KJPP wiring was used in cabinet fire experiments (experiments 2 and 3 in Mangs and Keski-Rahkonen 1994). The material supported flames and the total length burned out (group LB).

In the top figure in Figure 20, the series of tests using a single piece of MMO-A cable suspended vertically are plotted. A 70 mm high pilot flame was used for certain finite periods of time, and finally for the whole duration of the test. This cable configuration belongs clearly to group local spread (LS). In the middle of Figure 20, both the power of the pilot flame and configuration of the cable bundle were changed. Two pieces of MMAO-A cable still seemed to belong to LS group independent of pilot power used. Using four parallel cables suspended vertically side by side was the first configuration of MMO-A cable, which sustained flaming using a continuous 870 W pilot flame. In the bottom plot of Figure 20, MMO-A cables in single, double and four wire configurations were ignited using 1710 W pilot power. Double and quadruple configurations led to accelerating fire (LB).

In Figure 21 maximum possible heat release rates for tests plotted in Figure 20 are calculated from flaming length of cable and rate of heat release per unit area measured in cone calorimeter experiments. Since no heat release was measured in fast tests, these served as nominal dimensioning values for estimating ignition pilot size and cable configuration leading to accelerating ignition in electronic cabinet fire tests.

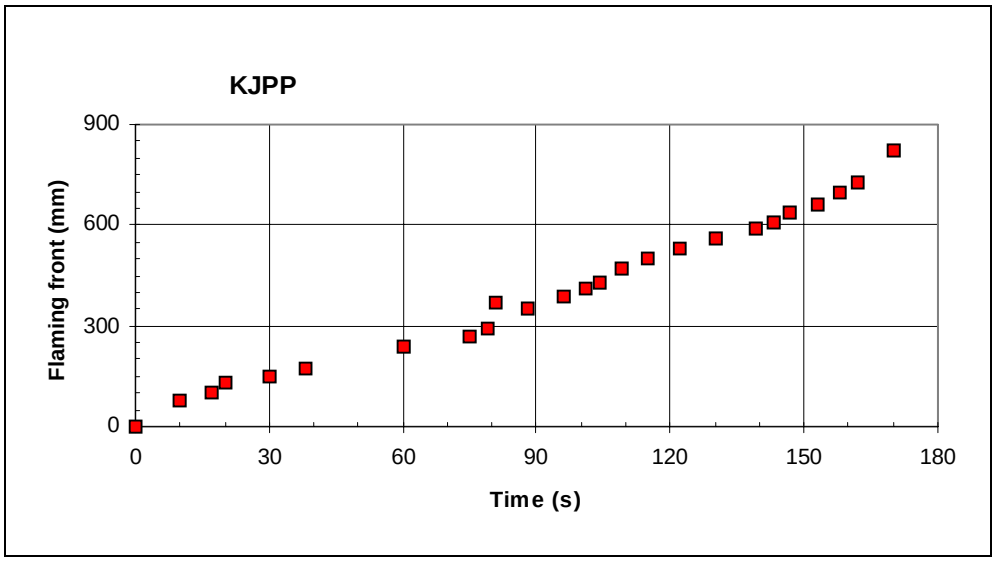

Figure 19. Spread of flaming front on cable KJPP ignited using a match.

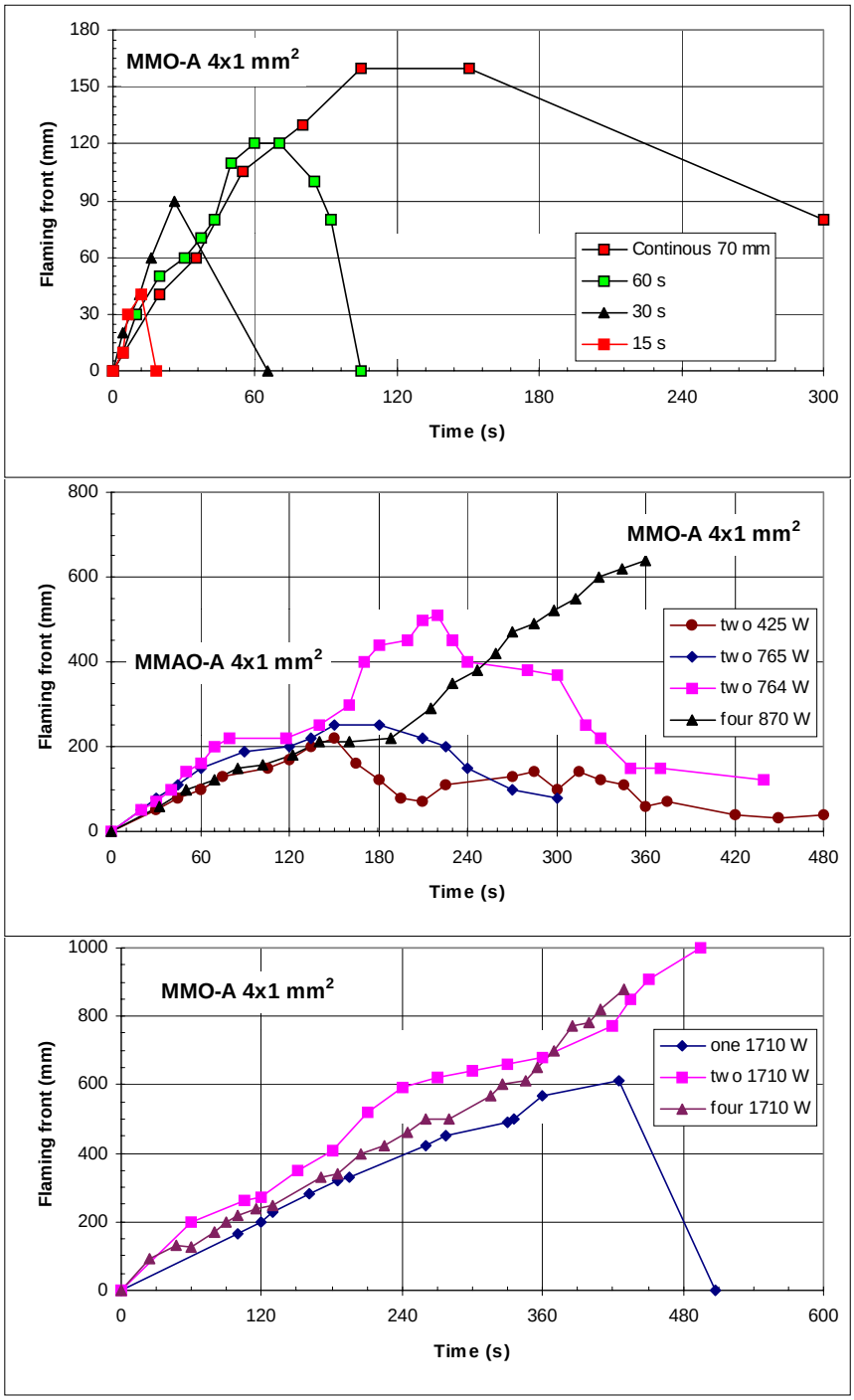

Figure 20. Spread of flame front on MMO-A and MMAO-A cables.

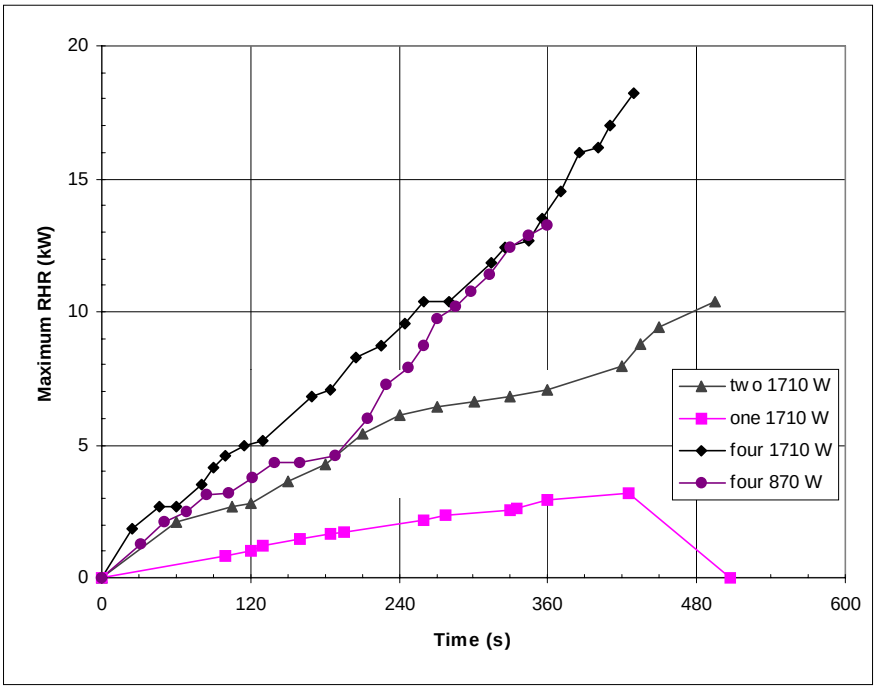

Figure 21. Maximum heat release rate from burning MMO-A cables.

We have carried out cone calorimeter experiments on cables, wires, and relays casings (Mangs & Keski-Rahkonen 1994, 1997). These tests measure ignition and burnoff times, and allow determination of heat release rates. Plotting the obtained data on the plane of Figure 18 allows the behaviour of the materials to be compared on a relative scale, LI, LS and LB. The ignition and spread times are much longer than the time needed to create ignition energy by a short circuit or ground fault.

If a LB ignition happens inside a cabinet, total heat release might exceed a critical threshold to cause a flashover (F). This would result in total burnout of all material in the cabinet. Using the experimental data obtained from burning of electronic cabinets (Mangs & Keski-Rahkonen 1994, 1996, Paananen 1996), a criterion for the lower threshold of flashover in a cabinet was established (Keski-Rahkonen & Mangs 1996). We have used these models, and rough experimental data of Figures 20 and 21 to design the size of the ignition source as well as the amount of material first ignited in such a way that theoretically predicted flashover threshold should be exceeded in a simulated cable tunnel fire (Mangs & Keski-Rahkonen 1997).

8 IGNITION OF A PRINTED CIRCUIT FROM AN OVERLOADED COMPONENT

A sample of 46 typical printed circuit boards (PCB) used at Finnish nuclear power plants were examined visually in order to find adequate components for fire experiments. Most of the components on the PCBs were integrated microcircuits such as logic circuits and memories. Most of the microcircuits were encapsulated in plastic. Only eight PCBs were purely analogue electronics without any digital components.

8.1 SELECTION OF COMPONENTS AND PRE-EXPERIMENTS

Typical components of the examined PCBs were microcircuits, capacitors, resistors and discrete semiconductor components such as transistors and diodes. Components were chosen for fire experiments using data books and previous knowledge. The main criteria were that the component can tolerate enough power (mainly current carrying capacity) for ignition to be possible or that it is a representive sample of all examined components.

The selected components were plastics encapsulated micro (logic) circuits, capacitors (tantalum, aluminium electrolyte and plastic film capacitors), resistors (metal film and bulk resistors) and power transistors in metal package (case type TO-3). All the selected components were packaged into via hole mount packages.

The basic material of printed circuit boards was glass fibre laminate (most likely type FR4). To find out the critical components, a series of pre-experiments was carried out.

8.1.1 Pre-experiments

Pre-experiments were made at VTT Automation to investigate whether the chosen components could ignite and to test how to introduce electric power to the components.

DC current and voltage were supplied to the components in both pre-experiments and fire experiments.

One typical medium size printed circuit board with digital electronics was selected from the sample of PCBs. The size of this PCB was 100 * 160 mm^2. The PCB was used to test microcircuits and both tantalum and plastic film capacitors. Test power was supplied to components using normal power and ground terminals of the PCB. Normal supply voltage to this PCB was 5 V.

Resistors and aluminium electrolyte capacitors were tested coupling the test power directly to the component. Power transistors were tested coupling the test power via bias resistor to the component.

The electrical stress supplied to the selected components was either overvoltage (or overcurrent) or faulty polarity of power supply.

8.1.2 Results from pre-experiments

The results of the pre-experiments are presented in Table 21.

Table 21. Summary of pre-experiments on electric components.

Component	**Test type**	**Measured value**	**Remarks**
Microcircuit	Overvoltage	Maximum used voltage 25 V	Microcircuits smoked during the test
Microcircuit	Faulty polarity of power supply	Maximum used voltage 8 V	Microcircuit "exploded"
Tantalum and plastic film capacitor	Overvoltage	Maximum used voltage 45 V	Tantalum capacitor started to burn
Tantalum and plastic film capacitor	Faulty polarity of power supply	Maximum used voltage 10 V	Tantalum capacitor sparkled -> short circuit -> smoke
Bulk resistor	Over power	Maximum used power 15 W	The component became warm
Metal film resistor	Over power	Maximum used power 4 W	The metal film was broken off because of the heat
Aluminium electrolyte capacitor	Faulty polarity of power supply	Maximum used voltage 60 V	Capacitor sparkled -> short circuit -> some smoke
Power transistor (BUX 42)	Constant power	Maximum used power 50 W	Transistor started to smoke

When overvoltage was supplied to microcircuits in the pre-experiments, components became warm (or even hot) and some light smoke from the capsulate of the component could be detected. Faulty polarity of power supply caused breakage of one plastic encapsulation. No flames were detected during the pre-test. Nominal supply voltage to the microcircuits was 5 V.

The voltage levels used in the pre-experiments caused no severe damage to plastic film capacitors. The nominal voltage of plastic film capacitors

was so high, typically an order of magnitude 100 V, that other components reacted before any limits were reached.

Faulty polarity of power supply caused no severe damage to aluminium electrolyte capacitors in the pre-experiments. Only some smoke could be detected, but no flames. Nominal voltage of the capacitors used was 33 V.

When overvoltage or faulty polarity of power supply was supplied to tantalum capacitors, both smoke and flames could be detected in the pre-experiments. Nominal voltage of the capacitors used was 25 V.

When overvoltage was supplied to resistors, only warming-up of the component was detected. For very high voltage the film inside the metal film resistor would break and after that no power could be supplied. A metal film resistor will act like a fuse in such situations. Only some smoke could be detected, but no flames. The maximum power of bulk resistors was 5 W and the maximum power of metal film resistors was 0.25 W.

When constant power was supplied to a power transistor, a lot of smoke could be detected. The package also became very hot. No limitation of supplying more power was detected, but the experiment was interrupted before any flames were detected because the facilities at VTT Automation are not suitable for fire experiments.

After the pre-experiments, a medium size PCB with microcircuits and tantalum capacitor was chosen for fire experiments. Power transistors were also chosen.

8.2 FIRE EXPERIMENTS

8.2.1 Experimental set-up and summary

The experiments were carried out under the hood of a cone calorimeter for rate of heat release measurements. Neither the external heat flux cone nor the spark ignitor of the cone calorimeter apparatus were used in the experiments. In each experiment one printed circuit board was in a vertical position under the hood and electric power was fed to it. A summary of the experiments is presented in Table 22 and they are described in detail in the text below.

Rate of heat release from oxygen consumption calorimetry, smoke production and sample mass were monitored as standard cone calorimeter measurements.

The electric power supplied to the components was monitored by measuring separately DC voltage and current values as calibrated output values of the connected power supply. Voltage and current values were observed visually from the display. The zero of the time scale used here corresponds to the beginning of the cone calorimeter measurements.

Nominal voltages of components mentioned in Section 8.1 are also applicable to components used in fire experiments.

Transistor BUX42 is a metal encapsulated (TO-3 case) power transistor (NPN) for switching purposes. The component can tolerate up to 12 A collector current (I_C) and minimum collector-emitter voltage (V_{CEO}) is 250 V. The component capsulate can tolerate 120 W, when the temperature is 25 °C. This means that all the generated heat must be transferred from the capsule. If the power transistor is designed to carry continuous high current, there must be some kind of heatsinks for the heat to be transferred from the capsule of the component. For switching purposes these are not normally used, because the component is scaled to tolerate maximum current and voltage at the switching moment. In continuous use the current and voltage levels are normally lower.

In these fire experiments the transistor would operate within an acceptable range of its voltage-current characteristics, if the temperature were 25 °C. However, the design of the printed circuit board does not allow the heat to transfer from the capsule. The only route for heat to transfer is via three soldered contacts. Continuous power in these experiments will raise the temperature of the encapsulated component. The only route for the heat from the capsule is via the pins of the capsule and after that via conductors of the PCB. This causes the temperature of these conductors to rise noticeably.

Power supplied to the component is mentioned when known. After damaging either components or wiring there was no current flow although voltage was supplied. In these cases only voltage values are mentioned with corresponding power < 1 W. Intermittent current peaks cannot be excluded, but could not be registered with the present equipment.

Rate of heat release clearly above noise level was recorded in experiments 7 and 8 only, in accordance with the visual observations of flames. Rate of heat release curves are presented for experiments 6, 7 and 8 in connection with the description of the corresponding experiment.

The sample mass measurements were disturbed by the connected electrical supply wiring, which slightly changed position during the experiments. The mass curves are therefore not presented because the small real changes in sample mass could not be clearly distinguished from changes induced by these disturbances.

No smoke production was detected in experiments 1 ... 3b. In experiments 4a ... 8, minor production of smoke was detected (Figure 32) with two distinct peaks corresponding to flaming of printed circuit board in experiments 7 and 8.

Table 22. Summary of fire experiments on electronic components.

Experiment	Object	Applied electric stress	Outcome of experiment
1	PCB board with microcircuits and tantalum capacitor	Overvoltage	One microcircuit flamed about 5 seconds, breaking of microcircuit and capacitor capsules, sparkling
2	PCB board with microcircuits and tantalum capacitor	Overvoltage	Tantalum capacitor flamed for about 30 s, sparkling
3a	PCB board with microcircuits and tantalum capacitor	Faulty polarity of power supply	Breaking of microcircuit and capacitor capsules, sparkling
3b	Same as 3a	Short circuit between power and ground terminal at one microcircuit socket	Slight smoke
4a	PCB board with microcircuits and tantalum capacitor	Faulty polarity of power supply	Flaming of the tantalum capacitor for about 20 s, flaming of a microcircuit for about 10 s., breaking of microcircuit capsules, sparkling
4b	Same as 4a	Short circuit between power and ground terminal at one microcircuit socket	Slight smoke
5	Tantalum capacitor	Overvoltage	Breaking of capacitor capsule
6	Power transistor BUX 42	Overcurrent	Smoke until glowing and breakage of emitter contact conductor
7	Power transistor BUX 42	Overcurrent	Flaming fire on PCB board surface for about 25 s
8	Power transistor BUX 42	Overcurrent	Flaming fire on PCB board surface for about 70 s

8.2.2 Fire experiments and results

Fire experiment 1: Overvoltage

Object: PCB board with microcircuits and tantalum capacitor

Size of PCB board: 100 * 160 mm^2

Course of events:

The input voltage was raised gradually (Figure 22). When the voltage level reached 26 V at 17.5 minutes, input current started to decrease. No reasons for this were detected visually, but the encapsulation of the microcircuit became warm.

At 34 minutes, 140 ^{o} C surface temperatures of hot microcircuits were measured with a K-type bare thermocouple. After 37.5 minutes from the start, the power supply was changed. At that point the voltage level was 35.8 V. After changing, the current decreased below 1 mA (P < 1 W).

When voltage level reached 49 V, one of the microcircuits ignited and burned for 5 s. When the voltage level reached 55 V, the tantalum capacitor sparkled. Voltage was raised up to 70 V, but no other effects were detected.

During the test the capsules of one microcircuit and the only tantalum capacitor broke down, but no damage was noticed in their surroundings.

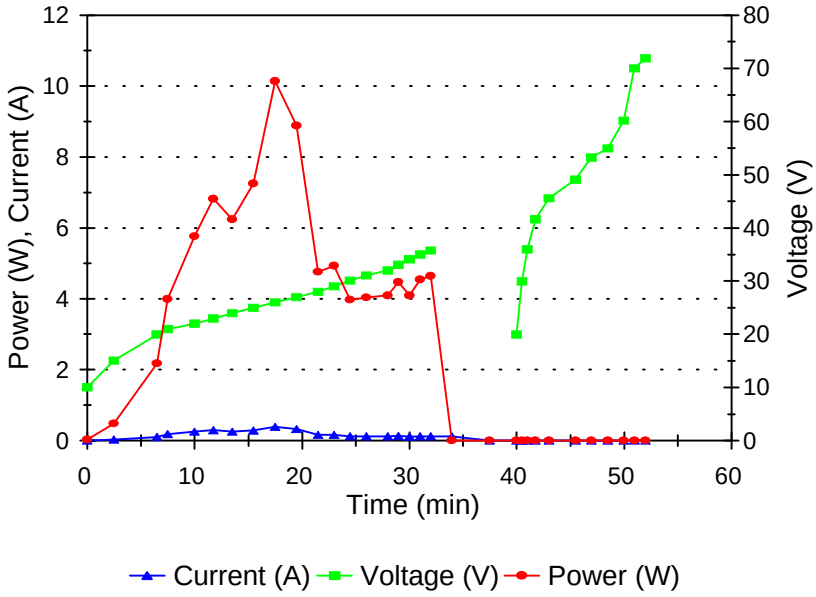

Figure 22. Electrical current, voltage and power supplied to PCB in component fire experiment 1. The power supply was changed between 37.5 and 40.0 min.

Fire experiment 2: Overvoltage

Object: PCB board with micro circuits and tantalum capacitor

Size of PCB board: 100 * 160 mm^2

Course of events:

The input voltage was raised gradually. When the voltage level reached 29 V, at 3.5 minutes, input current rose rapidly to 1 A and the voltage dropped to 5 V (Figure 23). No visual reasons were detected. At 5.75 minutes the capsule of one microcircuit started to smoke.

At 12 minutes the voltage level was raised rapidly. The input current started to oscillate and at 15 minutes the tantalum capacitor ignited (voltage 38 V) and the input current decreased below 1 mA (P < 1 W). The tantalum capacitor burned for about 30 s. At 16 minutes one

microcircuit started to sparkle (50 V) and after that the first microcircuit smoked some more (60 V). The voltage was raised to 70 V, but no other effects were detected in other components.

During the test the capsules of two microcircuits and the only tantalum capacitor broke down, but no damage was noticed in their surroundings.

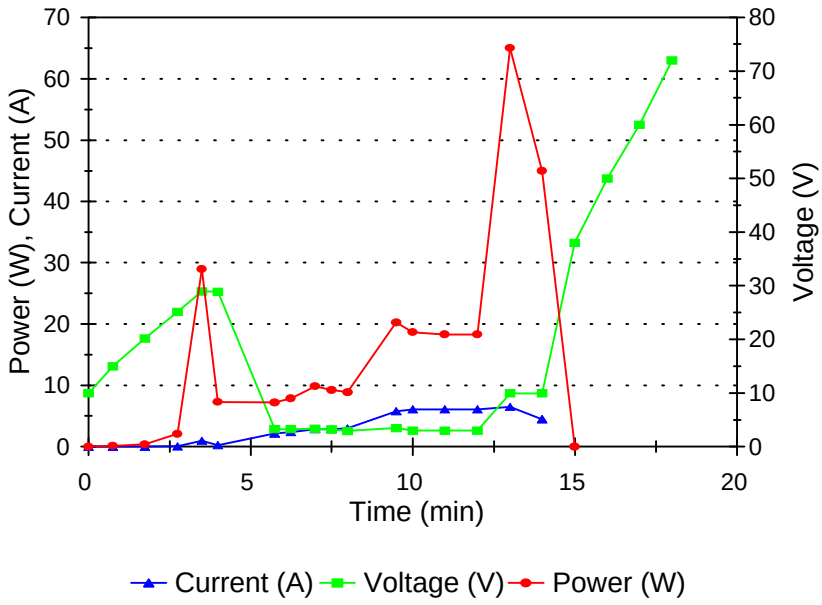

Figure 23. Electrical current, voltage and power supplied to PCB in component fire experiment 2.

Fire experiment 3a: Faulty polarity of power supply

Object: PCB board with microcircuits and tantalum capacitor

Size of PCB board: 100 * 160 mm^2

Course of events:

The input voltage was raised gradually. When the power level reached 34 W (8 A and 4.3 V) at 8 minutes, the capsule of one microcircuit started to smoke. After that the input current started to decrease (Figure 24). When

the voltage level reached 8 V, 12.5 minutes from the start, the tantalum capacitor capsule broke. After breakdown of the capacitor the current level decreased below 0.1 A.

After 15 minutes the voltage level was raised rapidly. When the voltage level reached 51 V the capsule of one microcircuit broke and when the voltage level reached 62 V capsules of two microcircuits started to flash. The voltage was raised to 72 V, but no other effects were detected in other components.

During experiment 3a three microcircuits and the only tantalum capacitor broke down, but no damage was noticed in their surroundings.

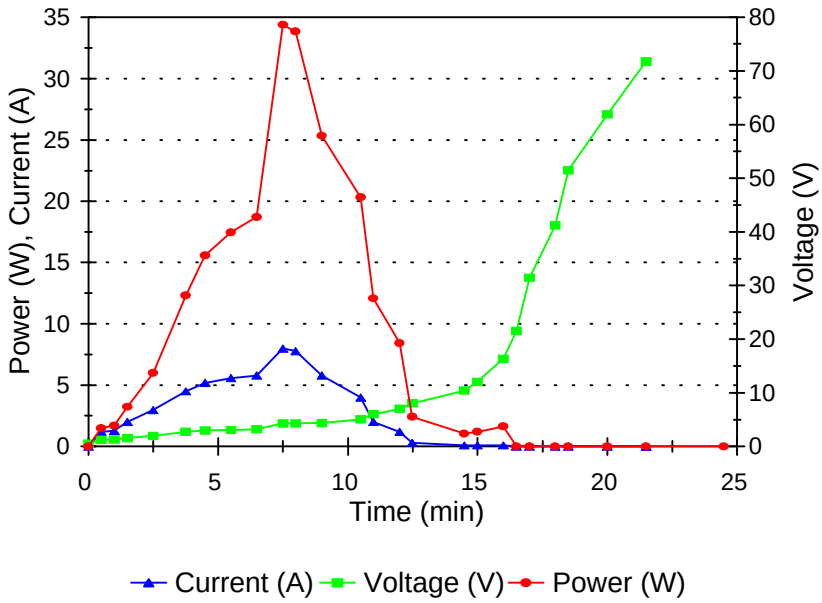

Figure 24. Electrical current, voltage and power supplied to PCB in component fire experiment 3a.

Fire experiment 3b: short circuit between power and ground terminal at one microcircuit socket

Object: Same PCB as in experiment 3a
Course of events:

The PCB from experiment 3a was also used to test the effects of short circuit between power and ground terminal at one microcircuit socket. The input power was raised very rapidly (Figure 25). At 3.5 minutes one capacitor started to smoke and at 4.5 minutes the conductor of the PCB broke due to overload.

The conductor of a PCB would act like a fuse in a situation like that. Only some smoke could be detected, but no flames.

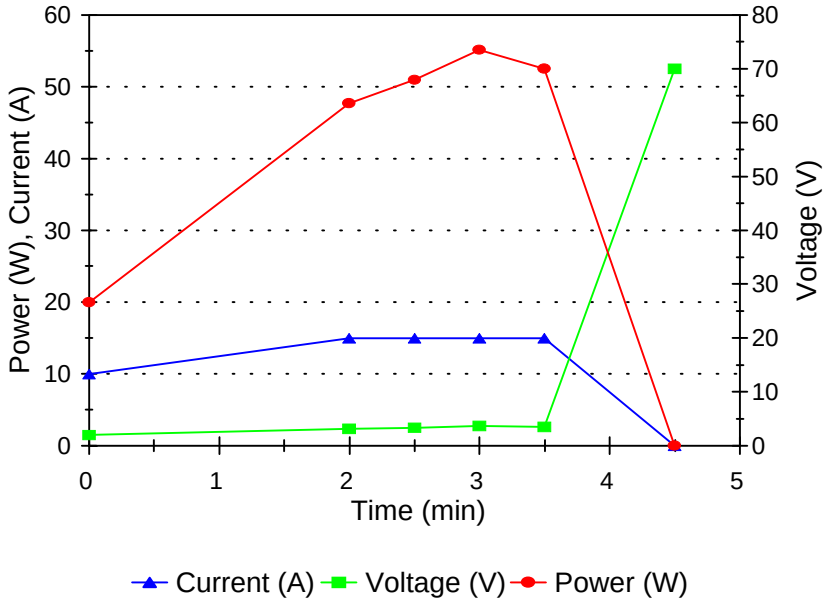

Figure 25. Electrical current, voltage and power supplied to PCB in component fire experiment 3b.

Fire experiment 4a: Faulty polarity of power supply

Object: PCB board with micro circuits and tantalum capacitor

Size of PCB board: 100 * 160 mm^2

Course of events:

The input voltage was raised gradually. When the power level reached 50 W (6 A and 8.4 V) at 9 minutes, the tantalum capacitor ignited. At the same time the input current decreased to 1 A (Figure 26). The capacitor burned for 20 s.

At 11 minutes the current level was raised rapidly from 0.2 to 3 A. When the current level reached 3 A at voltage 16 V (48 W) the capsule of one microcircuit flamed. At the same time the input current started to oscillate between 0.1 and 2 A. The capsule of one microcircuit started to spark. During that time the input current level decreased below 0.1 A.

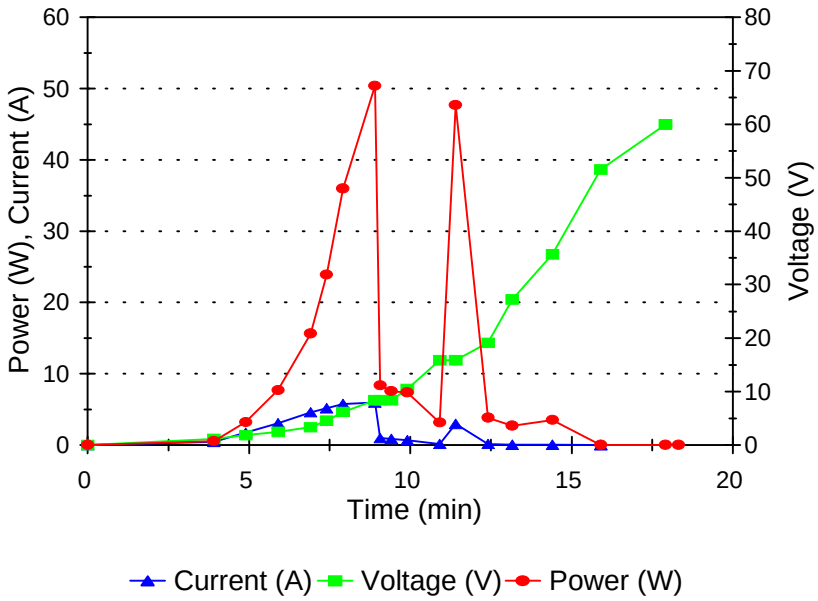

Figure 26. Electrical current, voltage and power supplied to PCB in component fire experiment 4a.

When the voltage level reached 52 V the capsule of one microcircuit "exploded" and when the voltage level reached 60 V capsules of four microcircuits started to spark for 20 s. The voltage was raised to 72 V, but no other effects were noticed at other components.

During the experiment six microcircuits and the only tantalum capacitor broke down, but no damage was noticed in their surroundings.

Fire experiment 4b: short circuit between power and ground terminal at one microcircuit socket

Object: Same PCB as in experiment 4a

Course of events:

The same PCB as in experiment 4a was also used to test the effects of a short circuit between power and ground terminal at one microcircuit socket. The input power was raised very rapidly in this experiment (Figure 27). Three minutes from the start some smoke was detected, but after that no other effects were detected.

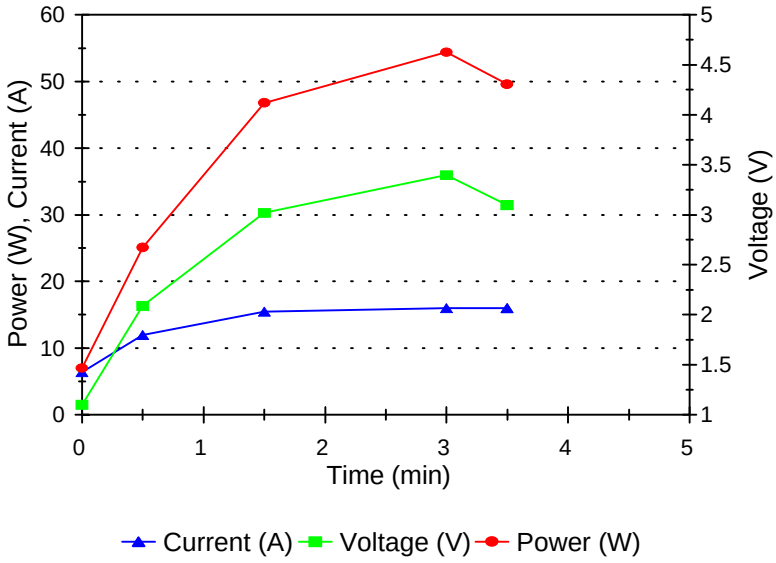

Figure 27. Electrical current, voltage and power supplied to PCB in component fire experiment 4b.

Fire experiment 5: Over voltage to tantalum capacitor

Object: PCB board with tantalum capacitor

Size of PCB board: 100 * 160 mm^2

Course of events:

The input voltage was raised rapidly. When the voltage level reached 58 V the tantalum capacitor "exploded". The voltage was raised to 72 V, but no other effects were detected. The input current was below 1 mA during the whole experiment.

Fire experiment 6: Continuous power to switching power transistor (BUX 42)

Object: PCB board with power transistor

Size of PCB board : 50 * 150 mm^2

Course of events:

In experiments 6, 7 and 8 input current was raised gradually, not voltage as in the PCB experiments. The input current was connected to the collector contact and the base contact was connected to this terminal via bias resistance (Figure 28). The input voltage and current values were monitored and the supplied power was calculated (Figure 29 a*)*. The experimental set-up was the same in experiments 6, 7 and 8.

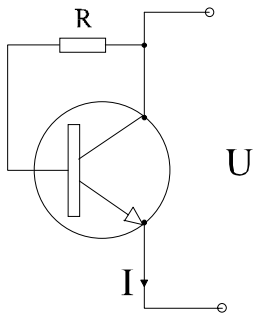

Figure 28. Coupling diagram of power transistor in experiments 6,7 and 8. R = 220 Ω.

When input power level reached 31 W (5.17 V and 6 A), 3 minutes from the start, the lacquer over the transistor started to fume. When the current was raised to 7 A (38.5 W), 5 minutes from the start, voltage level started to decrease. After a few moments the voltage level stabilised (29 W). This happened every time (in tests 6...8) when the current level was raised.

After the input current was raised to 9 A and the voltage were stabilised to 4 V (36 W), at 9 minutes, the surroundings of the power transistor started to fume for about 20 s. Every time power was raised to a new level, some more lacquer (or other surface material) was volatilised over a large area of PCB.

When the power level exceeded 50 W the conductor to emitter contact started to glow. At 16.3 minutes from the start, the conductor finally broke.

Rate of heat release during the experiment is presented in Figure 29 b together with supplied electric power.

After the experiment the damaged area of the PCB was measured. On the bottom the area was oval shaped (60 * 25 mm^2) and on the upper side the area was oval (10 * 15 mm^2) around the collector terminal. All surface material coating the conductor to emitter was volatilised at 45 mm distance.

a)

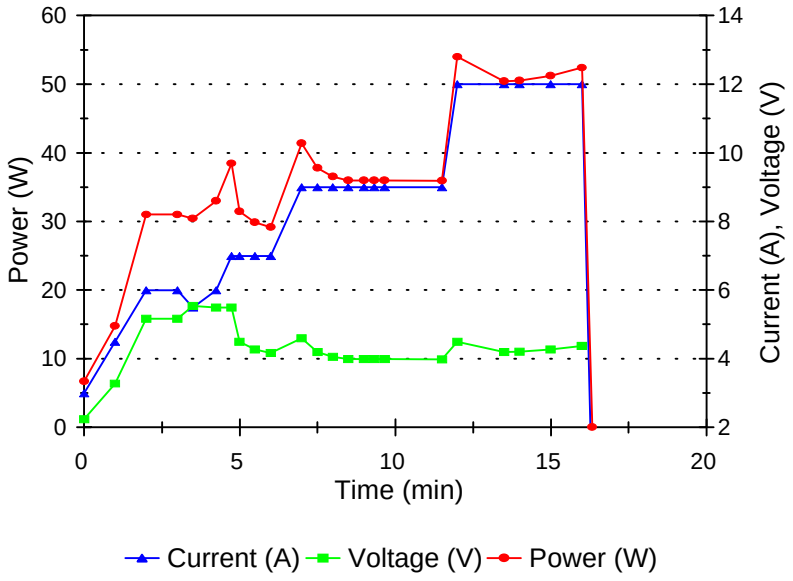

b)

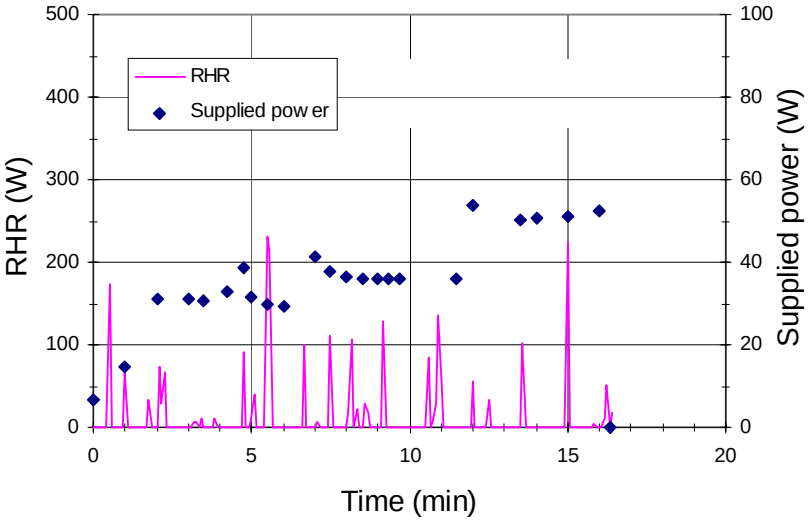

Figure 29. a) electrical current, voltage and power supplied to transistor in component fire experiment 6, b) rate of heat release from and electrical power supplied to transistor in component fire experiment 6.

Fire experiment 7: Continuous power to switching power transistor (BUX 42)

Object: PCB board with power transistor

Size of PCB board: 45 * 150 mm^2

Course of events:

The input current was raised gradually. When input power level reached 43 W (6.2 V and 7 A), 1 minute from the start, lacquer over the transistor started to fume. The power level was kept over 40 W, but no effects were noticed (Figure 30 a).

When current was raised to 15 A (75W), 19.5 minutes from the start, the PCB started to burn. After 27 s the emitter contact broke because of the heat.

Rate of heat release during the experiment is presented in Figure 30 b together with electric power supplied.

After the experiment the damaged areas of the PCB were measured. On the bottom the area was about size 75 * 35 mm^2 and on the upper side the area was about size 75 * 40 mm^2. The surface area around the conductor to emitter was burnt at 55 mm distance (10 mm wide).

a)

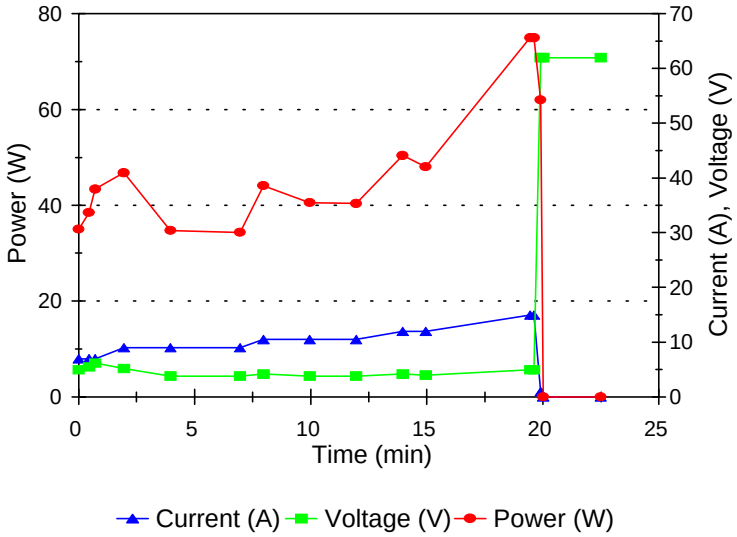

b)

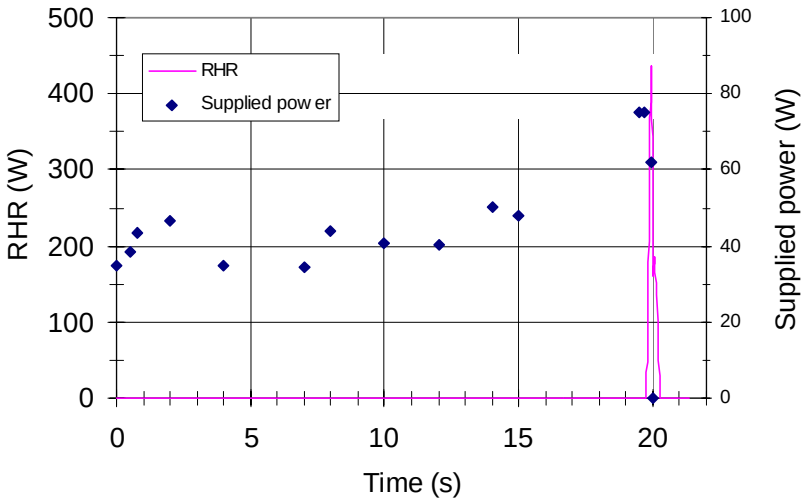

Figure 30. a) electrical current, voltage and power supplied to transistor in component fire experiment 7, a) rate of heat release from and electrical power supplied to transistor in component fire experiment 7.

Fire experiment 8: Continuous power to switching power transistor (BUX 42)

Object: PCB board with power transistor

Size of PCB board: 45 * 150 mm^2

Course of events:

The input current was raised gradually. When input power level reached 32 W (5.4 V and 6 A), 2 minutes from the start, lacquer over the transistor started to fume. At 6.75 minutes the solder of the emitter connection started to melt (power = 40 W). This means that the temperature must exceed 180 °C. The power level was kept around 60 W, but no effects were noticed (Figure 31 a).

When the current was raised to 15 A at time 14.25 minutes, voltage jumped over 6 V (93 W), and the PCB started to fume a lot. Then the current dropped and started to oscillate between 0.1 and 3 A and the voltage rose to 40 V. The PCB started to burn, 14.3 minutes from the start, voltage level rose to 70 V and maximum current level decreased to 1 A. The PCB burned for about 70 s, and stopped as the input cables broke because of the heat.

Rate of heat release during the experiment is presented in Figure 31 b together with electric power supplied.

After the experiment the damaged area of the PCB was measured. On the bottom the damaged area was about size 65 * 45 mm^2 and on the upper side the damaged area was about size 75 * 45 mm^2. The charred area on the bottom was about 25 * 40 mm^2 and on the upper side about size 20 * 45 mm^2. In the burned area all the surface materials were volatilised over the base laminate of the printed circuit board.

a)

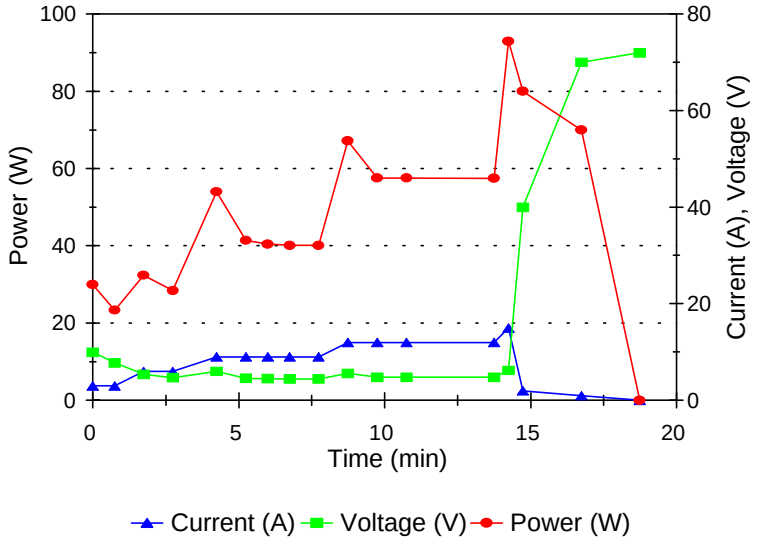

b)

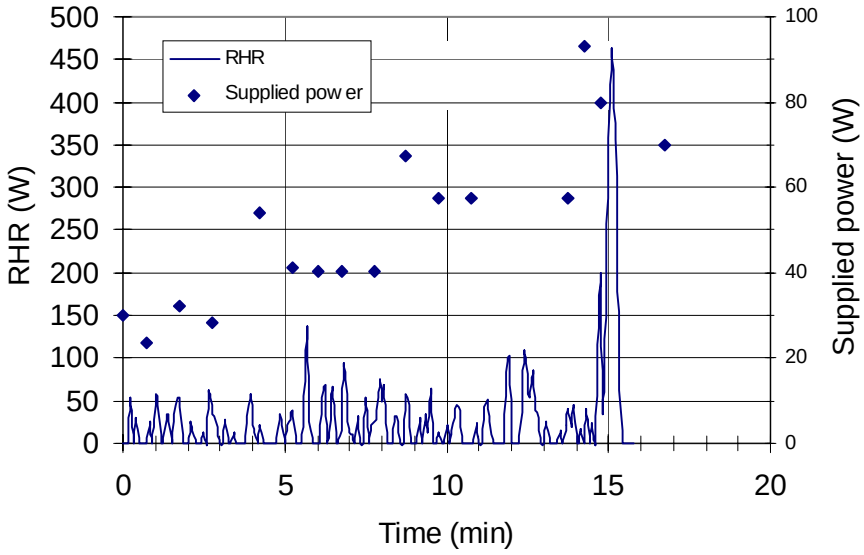

Figure 31. a) electrical current, voltage and power supplied to transistor in component fire experiment 8, a) rate of heat release from and electrical power supplied to transistor in component fire experiment 8.

Smoke production

Smoke production was measured from the damping of a He-Ne laser light beam in the exhaust duct of the cone calorimeter. The smoke production rate R is here calculated as

$$R = \dot{V}k \tag{77}$$

where $\dot{V}$ is volume exhaust flow rate measured at the location of the laser photometer and the extinction coefficient k is defined as

$$k = \frac{1}{L}\ln(\frac{I_0}{I}) \tag{78}$$

where I_o is beam intensity in smoke free environment and I is beam intensity after traversing a certain length L in smoky environment.

Smoke production rates measured in experiments 4a ... 8 are presented in Figure 32. No damping of the laser beam was detected in experiments 1 ... 3b.

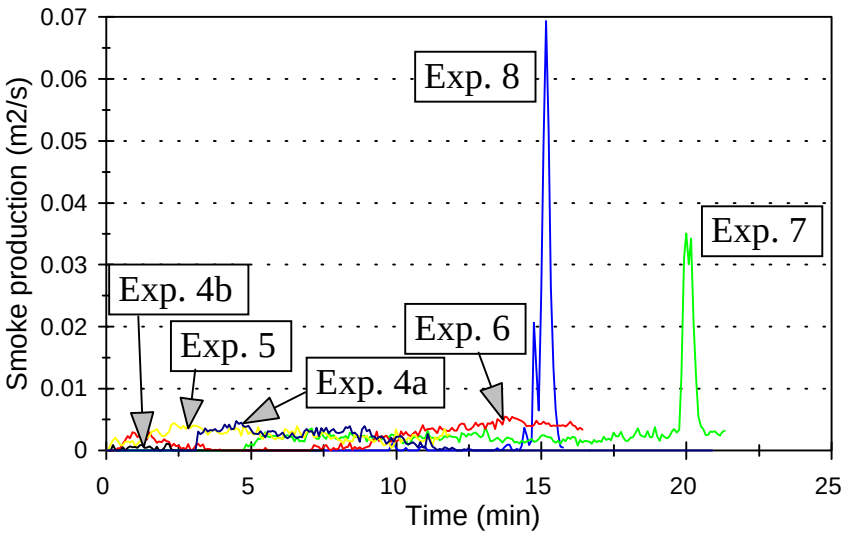

Figure 32. Smoke production rate in component fire experiments 4a ... 8.

8.3 CONCLUSIONS FROM COMPONENT FIRE EXPERIMENTS

Three experiments were carried out with power transistors. The surface of the printed circuit board ignited in two experiments, leading to distinct flaming fires lasting 25 and 70 s, respectively. The flames went out when the conductor to the transistor broke due to overloading. Maximum rate of heat release was 450 W in these power transistor experiments.

Seven experiments were carried out with microcircuits and tantalum capacitors. Capsules of microcircuits and tantalum capacitors ignited and burned with a small flame for 5 ... 30 s in some of the experiments without igniting adjacent components or circuit board. The rates of heat released from these components were below the detection level of the cone calorimeter. Other observed effects on microcircuits and capacitors were sparking, slight smoke production and breaking of component capsules.

The experiments indicate that, of the present components, the power transistor was the only component with potential to ignite adjacent combustible material.

9 CONCLUSIONS

This paper reviews electrical ignition phenomena from a wide perspective through statistical, modelling and experimental tools. It is believed a rather comprehensive concept of electrical ignition phenomena has been described. Many of the detailed conclusions drawn are given in the text in the relevant positions and are not repeated here. Several databases indicate that defective cables leading to short circuit and ground shorts, as well as loose connections leading to overheating, are the most common reasons for electrical ignitions.

For modelling an overheated cable, a mathematical model has been proposed which compares favourably with a limited set of experimental data, but can be applied only at rather low temperatures as compared to the melting temperature of cable insulation. Self-heating of cables is described using existing theory. Experiments on PVC cables showed it to be a possible but an improbable cause of initial ignition.

The literature review of physical models of electrical arcs established conditions where ignition of cables might be possible. A limited set of tests under poorly controlled conditions did not succeed in producing long lasting arcs amenable to sustained ignition. This is in contrast to observations from databases where arcing is one of the important causes of ignition. The reason for experimental failure is believed to be too violent release of energy, which blew off the flames.

Existing semiquantitative models of flame spread are shown to be able to describe salient features of cable ignitions despite clear deviations of initial assumptions of the model. Because of the importance of cable-originated ignitions for fire safety, and the promising theoretical results, continuing experimental and theoretical work on modelling cable ignitions and flame spread on cables would be desirable.

Laboratory tests of electronic components heavily or destructively overloaded did not generally lead to ignition of adjacent material because of sudden release of electrical energy and subsequent destruction of the component. Only power transistors heavily mounted on printed cards seemed able to start ignition of the card. The phenomenon can be modelled as a piloted ignition similar to flame spread on cables.

REFERENCES

Arfken, G. 1985. Mathematical methods for physicists, Third Edition. Orlando: Academic Press. 985 p.

Abramowitz, M. & Stegun, I.A. 1972. Handbook of mathematical functions. New York: Dover. 1046 p.

Ayrton, H. 1895. The Electric Arc. The Electrician 35, p. 419.

Baroudi, D. & Kokkala, M. 1992. Analysis of Upward Flame Spread. Espoo: Technical Research Centre of Finland. 49 p. (VTT Publications 89)

Björkman, J. & Keski-Rahkonen, O. 1992. Test method for self-ignition of materials. Espoo: Technical Research Centre of Finland. 28 p + app. 13 p. (VTT Publications 96).

Bowes, P.C. 1974. Fires in oil-soaked lagging, Fire Prevention Science and Technology, No 9, p.13 - 22.

Bowes, P.C. & Langford, P. 1968. Spontaneous ignition of oil-soaked lagging. Chemical and Process Engineering, vol. 49, no 5, p. 108 - 116.

Bowes, P.C. 1984. Self-heating: evaluating and controlling the hazards. London: Department of the Environment, Building Research Establishment, Her Majesty´s Stationery Office. 500 p.

Chambré, P.L. 1952. On the solution of the Poisson-Boltzmann equation with applications to the theory of thermal explosions. The Journal of Chemical Physics, vol. 20, no 11, p. 1795 - 1797.

CRC 1984. CRC Handbook of Chemistry and Physics, CRC Press, Boca Raton, FA, 65th Edition.

Dekker, A.J. 1964. Solid State Physics. London: Macmillan. 540 p.

Delichatsios, M.A. & Delichatsios, M.M. 1994. Upward Flame Spread and Critical Conditions for PE/PVC Cables in a Tray Configuration, in Fire Safety Science - Proceedings of the Fourth International Symposium,

T. Kashiwagi (ed.), International Association of Fire Safety Science, Gaithersburg, 1994. Pp. 433 - 444.

Finkelnburg, W. 1948. Hochstromkohlebogen. Berlin: Springer 221 p.

Finkelnburg, W. & Maecker, H. 1956. Elektrische Bögen und thermisches Plasma. In S. Flügge (ed.). Handbuch der Physik, Band XXII. Berlin: Springer. Pp. 254 - 444.

Gomberg, A. & Hall, J.R. 1983. Analysis of electrical fire investigations in ten cities. NBSIR 83-2677. Gaithersburg, MD: National Bureau of Standards. 57 p.

Gradsteyn, I.S. & Ryzhik, I.M. 1983. Table of integrals, series, and products. New York: Academic Press. 1160 p.

Gray, B.F., Dewynne, J., Hood, M. Wake, G.C. & Weber, R. 1990. Effect of deposition of combustible matter onto electric power cables. Fire Safety Journal, vol. 16, pp. 459 - 467.

Gross, D. 1985. Data sources for parameters used in predictive modeling of fire growth and smoke spread, NBSIR 85-3223. Gaithersburg, MD: National Bureau of Standards. 40 p.

Hagenbach, A. 1927. Der elektrische Lichtbogen. In: H. Geiger and K. Scheel (eds.) Handbuch der Physik, Band XIV. Berlin: Springer. Pp. 324 - 353.

Hasemi, Y. 1986. Thermal Modeling of Upward Wall Flame Spread, In: Fire Safety Science - Proceedings of the First International Symposium, C.E. Grant, and P.J. Pagni (eds.), Hemisphere, Washington, D.C. 1991, Pp 87 - 96.

Hasemi, Y., Yoshida, M., Yasui, N. & Parker, W.J. 1994. Upward Flame Spread Along a Vertical Solid for Transient Local Heat Release Rate, in in Fire Safety Science - Proceedings of the Fourth International Symposium, T. Kashiwagi (ed.), International Association of Fire Safety Science, Gaithersburg, 1994. Pp 385 - 396.

International Atomic Energy Agency (IAEA). 1997. Advanced Incident Reporting System (AIRS) Database, October 1997 release of version 1.1. Vienna, Austria: International Atomic Energy Agency. CD-ROM.

Ivannikov, V.L. & Zernov, S.I. 1990. Metoditseskie osnovy ekspertnoj ochnki pozharnoj bezopasnosti kabel'nyh kommunikachij atomnyh stanchij [Basic methods for assessing fire safety of cable connections in nuclear power plants], Kiev: Ministry of atomic energy of USSR. 172 p. (in Russian).

Kohn, H., & Guckel, M. 1924. Untersuchungen am Kohlelichtbogen; Dampfdruckbestimmungen des Kohlenstoffs, Zeitschrift für Physik 27, pp. 305 - 357.

Keski-Rahkonen, O. & Mangs, J., 1996. Maximum and minimum rate of heat release during flashover in electronic cabinets of NPPs, in Faillace, R., Müller, K., Röwekamp, M. & Schneider, U (ed.), Proceedings of SMiRT 13 Post Conference Seminar No. 6, August 21-24, 1995, Fourth International Seminar on Fire Safety in Power Plants and Industrial Installations, Gramado, Brasil. SR 2092 / INT 9047, GRS-V-Bericht 9, 1996. Pp. 19-31.

Kunkel, W.B. 1966. Plasma physics in theory and application. New York: McGraw-Hill. 494 p.

Lees, F. P. 1980. Loss prevention in the process industries, Volume 1. London: Butterworths. 671 p.

Madden, P.M. Fire safety rulemaking issues confronting regulatory change in the United States. SMiRT 14, Fifth Post Conference Seminar n:o 6: Fire Safety in Nuclear Power Plants and Installations. Lyon, France, 25. - 29.8 1997. 18 s.

Mangs, J. & Keski-Rahkonen, O. 1994. Full scale fire experiments on electronic cabinets, VTT Publications 186, Technical Research Center of Finland, Espoo, 50 p. + app. 37 p.

Mangs, J. & Keski-Rahkonen, O. 1996. Full scale fire experiments on electronic cabinets II, VTT Publications 269, Technical Research Center of Finland, Espoo, 48 p. + app. 6 p.

Mangs, J. & Keski-Rahkonen, O. 1997. Full scale fire experiments on vertical and horizontal cable trays, VTT Publications 324, Technical Research Center of Finland, Espoo, 58 p. + app. 44 p.

Maxfield, F.A. & Benedict, R.R. 1941. Theory of gaseous conduction and electronics. New York: McGraw-Hill. 483 p.

Meek, J.M. & Craggs, J.D. 1953. Electrical breakdown of gases. Oxford: Clarendon Press. 507 p.

Miller, A. 1994. Selections from the U.S. Home Product Reports. 1988-1992 (Appliances and Equipment). Quincy, MA, National Fire Protection Association.

Paananen, J., 1996. Instrumenttikaapin palon suurimman tehon kokeellinen määritys [Experimental determination of the maximum rate of heat release of an electronic cabinet]. Master's thesis. Helsinki University of Technology. Structural Engineering and Building Physics, Fire and Safety Engineering 1996. 111 p. + app. 22 p. (in Finnish)

Quintiere, J.Q. & Lee, C.H. 1998. Ignitor and Thickness Effects on Upward Flame Spread, Fire Technology 34, pp 18 - 38.

Saito, K., Quintiere, J.G., & Williams, F.A. 1986. Upward Turbulent Flame Spread, in Fire Safety Science - Proceedings of the First International Symposium, C.E. Grant, and P.J. Pagni (eds.), Hemisphere, Washington, D.C. 1991, pp 75 - 86.

Smelkov, G.I. 1992. O kontseptsii pozharnoj besopasnosti elektritšeskih izdelij [On the conception of fire safety of electrotechnical products, electronic equipment and computer facilities]. Pozarovzryvobezopasnost, vol 1, no 2, pp. 28 - 32. (In Russian)

Smelkov, G.I. 1993. Statistitšeskie dannye o pozharnoj opasnosti elektritšeskih izdelij v 1992 godu [Statistical data on fire hazard of electrical products]. Pozarovzryvobezopasnost, vol 2, no 4, pp. 21 - 24. (In Russian)

Smelkov, G.I. & Pekhotikov, V.A. 1996. Problemy verojatnostnoj otsenki pozharnoj opasnosti elektritšeskih izdelij pri sertifikatsionnyh ispytanija [Problems of evaluation of fire hazard probability for electric hardware

during certification tests]. Pozarovzryvobezopasnost, vol 5, no 1, pp. 47 - 50. (In Russian)

Smelkov, G.I. & Pekhotikov, V.A. 1997. On the assessment of an electrical fire risk. In: Fire and explosion hazard of substances and venting of deflagrations. Second international seminar 11 - 15 August, 1997, Moscow, Russia. Pp. 97 - 99.

Smelkov, G.I., Pekhotikov, V.A., Teskin, O.I. & Oberfeld, G.Ya. 1995. Soveršenstvovanie metodov verojatnostnoj otsenki pozharnoj opasnosti elektritšeskih izdelij [Advancement of methods for probabilistic estimation of fire hazard of electrical products]. Pozarovzryvobezopasnost, vol 4, no 3, pp. 5 - 9. (In Russian)

Tamminen, A. 1996. Sähköpalojen henkilö- ja omaisuusvahingot. Master's thesis. Tampere University of Technology, Department of Electrical Engineering. 84 p. + app. 7 p. (in Finnish)

Thomas, P.H. 1958. On the thermal conduction equation for self-heating materials with surface cooling. Transactions of the Faraday Society, vol. 54, pp. 60-65.

Thomas, P.H. & Bowes, P.C. 1961. Some aspects of the self-heating and ignition of solid cellulosic materials, British Journal of Applied Physics, vol. 12, pp. 222 - 229.

Thomas, P. & Karlsson, B. 1990. On Upward Flame Spread on Thick Fuels, SE-LUTVDG/TVBB-3058, Department of Fire Safety Engineering, Lund University, 22 p.

U.S. Consumer product safety comission 1992. Electrical fire losses 1990. U.S. Consumer product safety comission, memorandum.

Vilyunov, V.N. & Zarko, V.E. 1989. Ignition of solids. Amsterdam: Elsevier. 441 p.

Weitzel, W. & Rompe, R. 1949. Theorie elektrischer Lichtbögen und Funken. Leipzig: J.A. Barth. 132 p.

Welty, J.R., Wicks, C.E. & Wilson, R.E. 1984. Fundamentals of momentum, heat, and mass transfer, third edition. New York: Wiley. 803 p.

Wheelis, W.T. 1986. Users' guide for a personal-computer-based nuclear power plant fire data base. Albuquerque: Sandia National Laboratories. 181 p. (NUREG/CR-4586, SAND86-0300).

Özisik, M.N. 1980. Heat conduction. New York: Wiley. 687 p.

Temperatures in experiments on heating of cables with electrical current

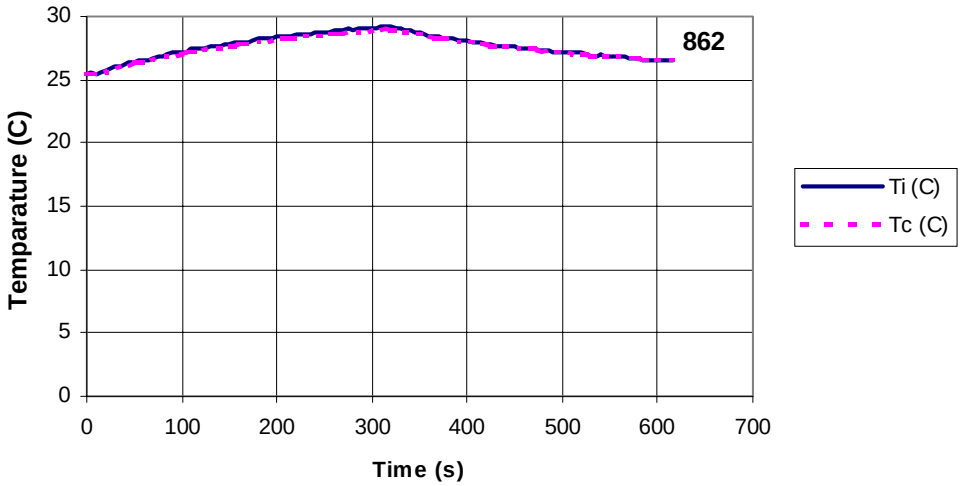

Figure 1. Temperatures in cable heating experiment 1.

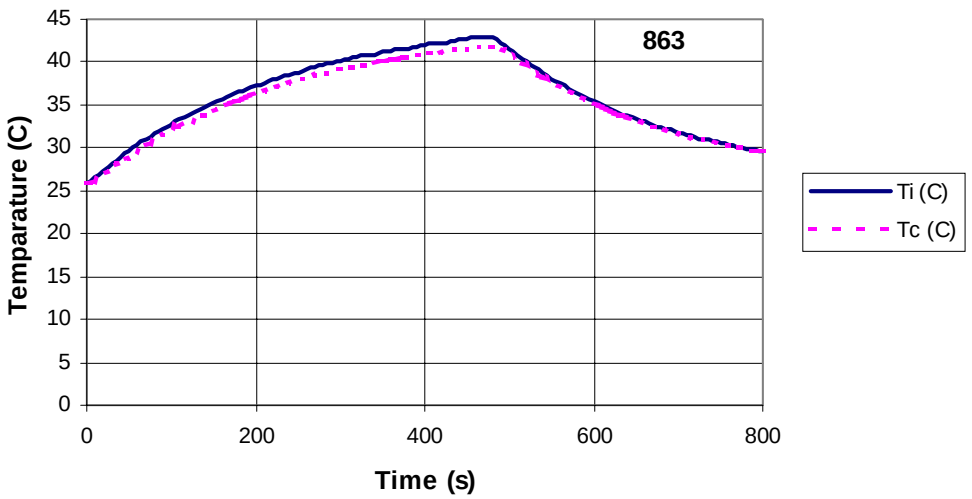

Figure 2. Temperatures in cable heating experiment 2.

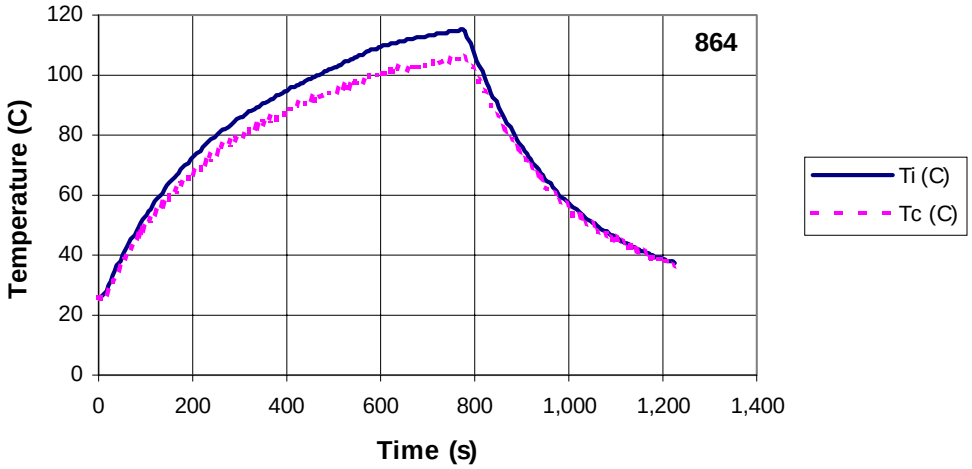

Figure 3. Temperatures in cable heating experiment 3.

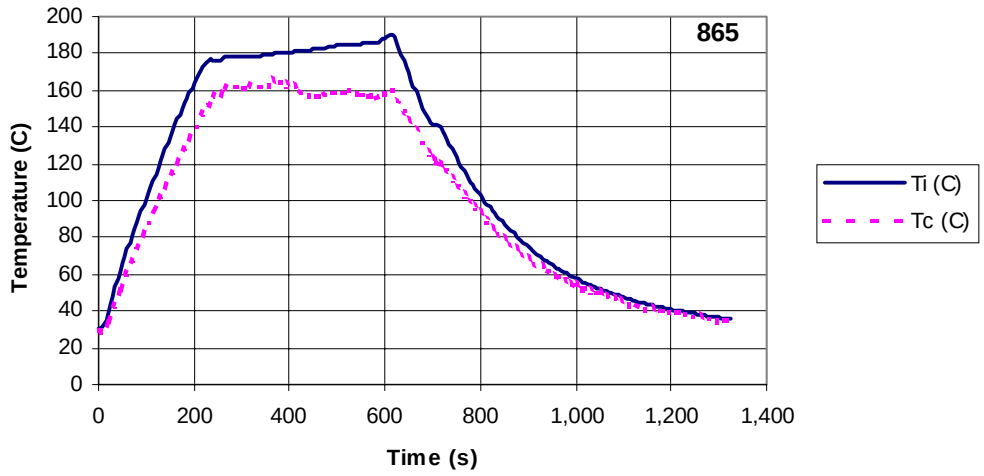

Figure 4. Temperatures in cable heating experiment 4.

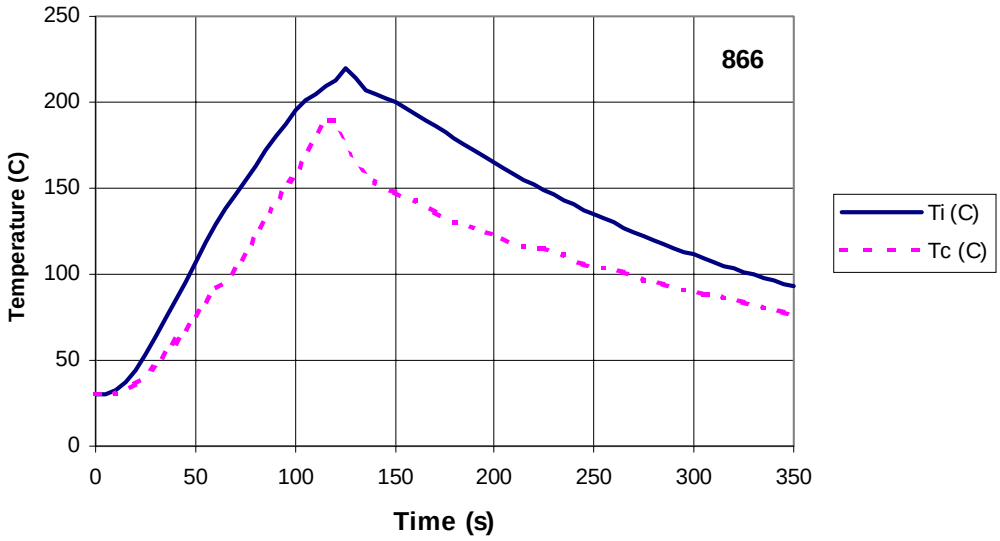

Figure 5. Temperatures in cable heating experiment 5.

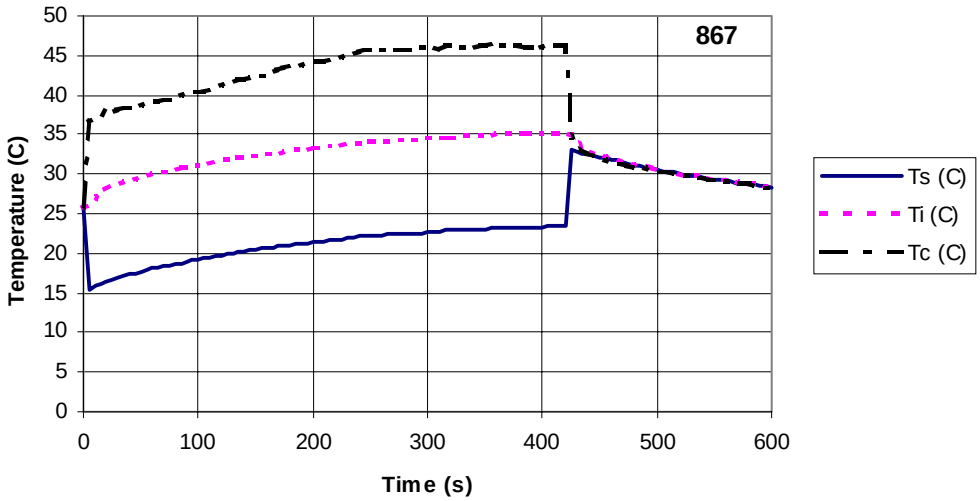

Figure 6. Temperatures in cable heating experiment 6.

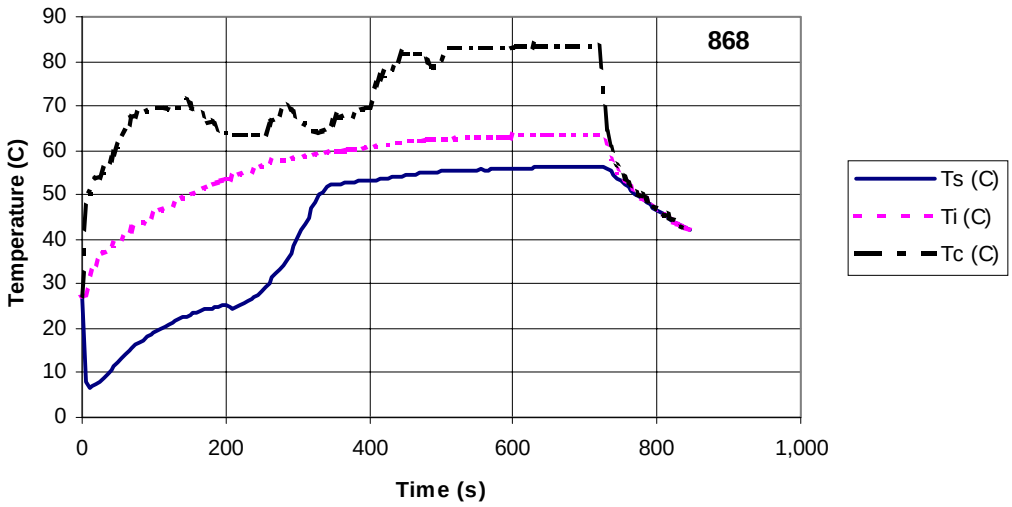

Figure 7. Temperatures in cable heating experiment 7.

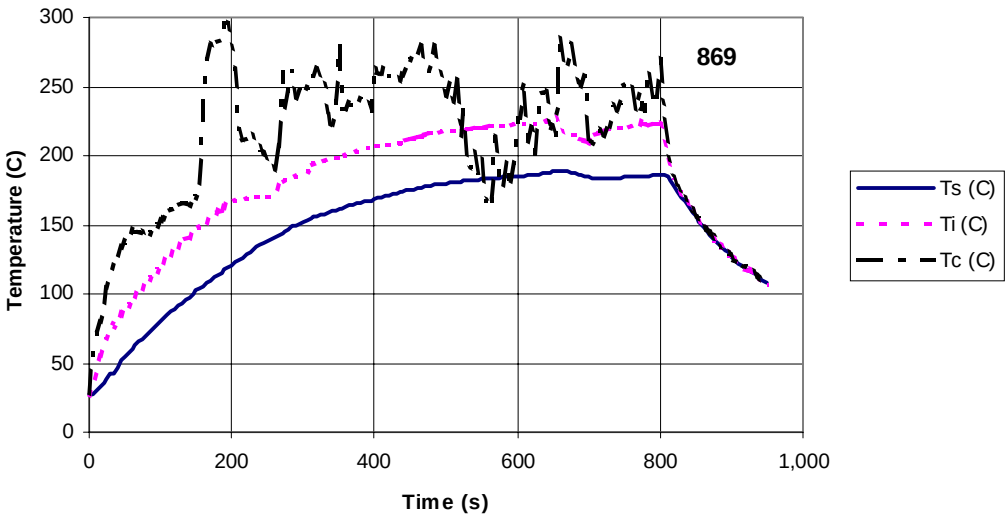

Figure 8. Temperatures in cable heating experiment 8.

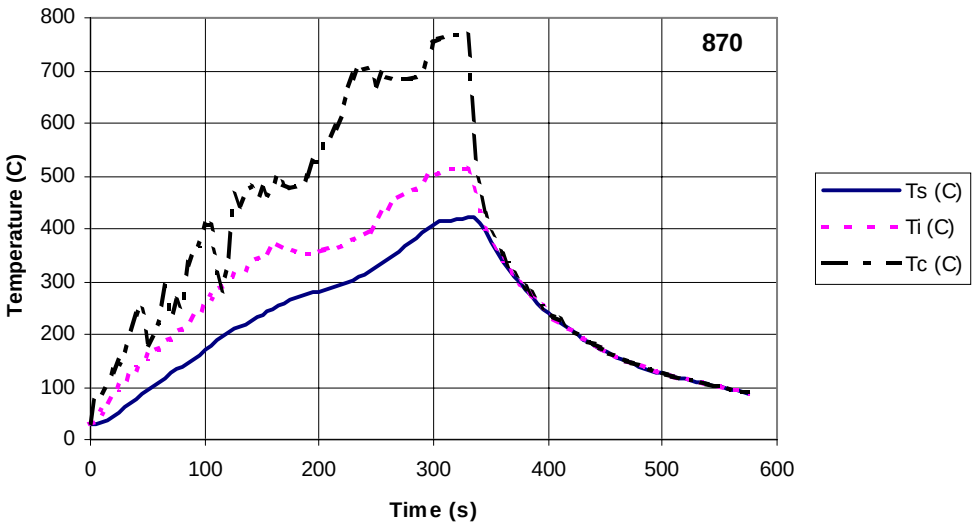

Figure 9. Temperatures in cable heating experiment 9.

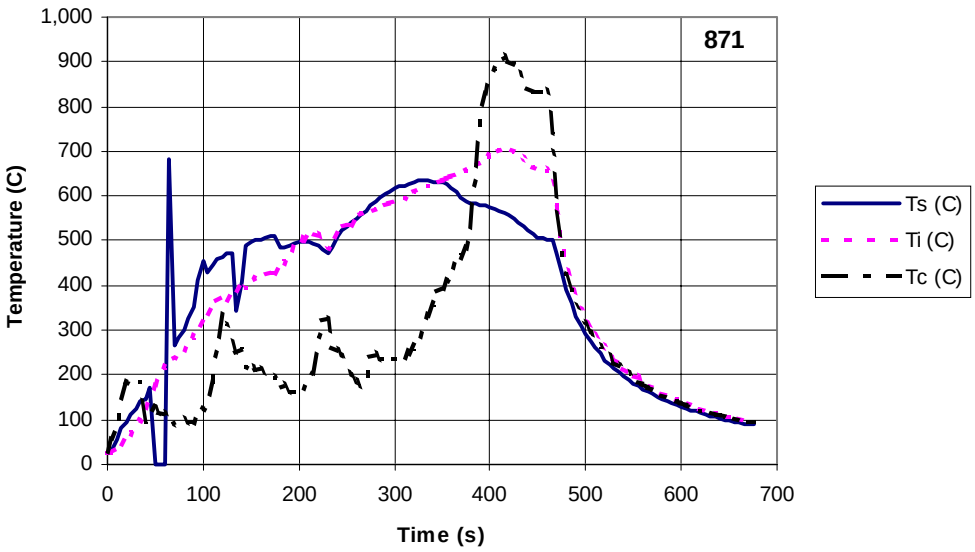

Figure 10. Temperatures in cable heating experiment 10.

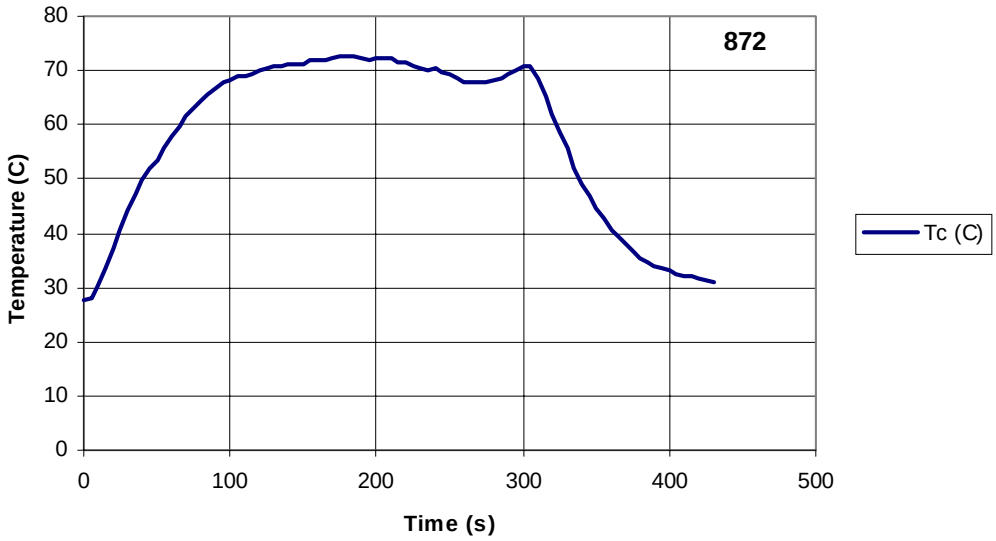

Figure 11. Temperatures in cable heating experiment 11.

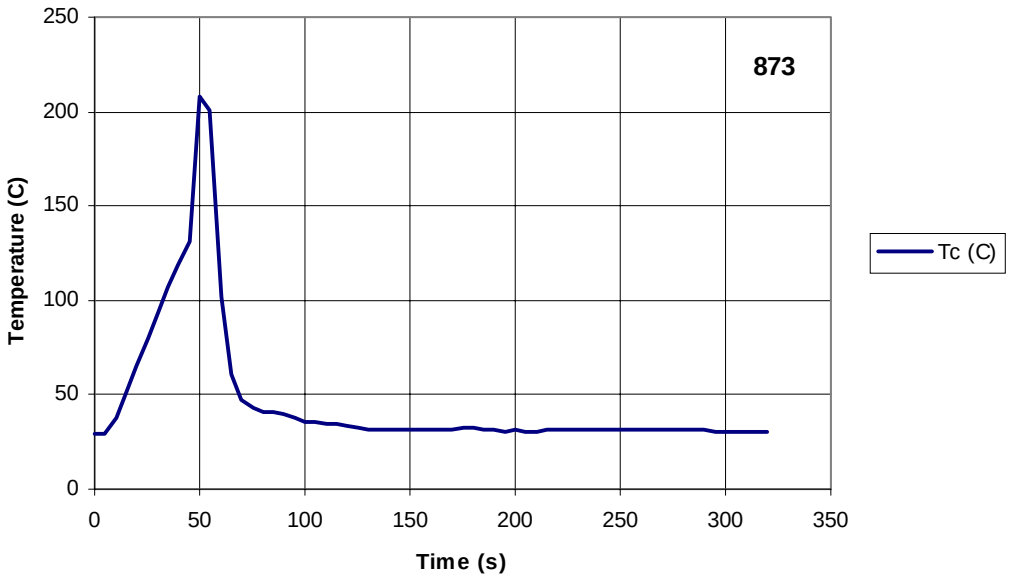

Figure 12. Temperatures in cable heating experiment 12.

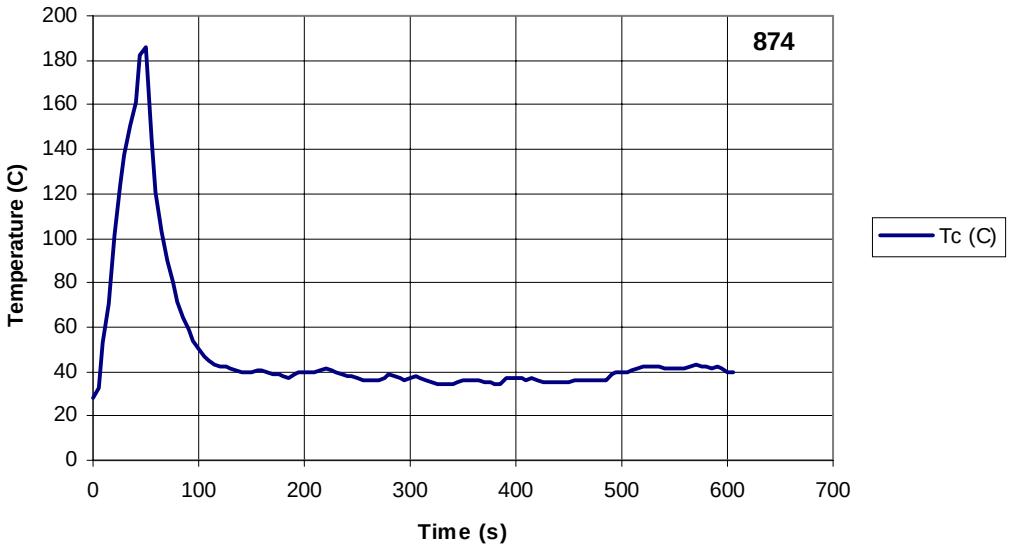

Figure 13. Temperatures in cable heating experiment 13.

Cable self-ignition test temperatures

a)

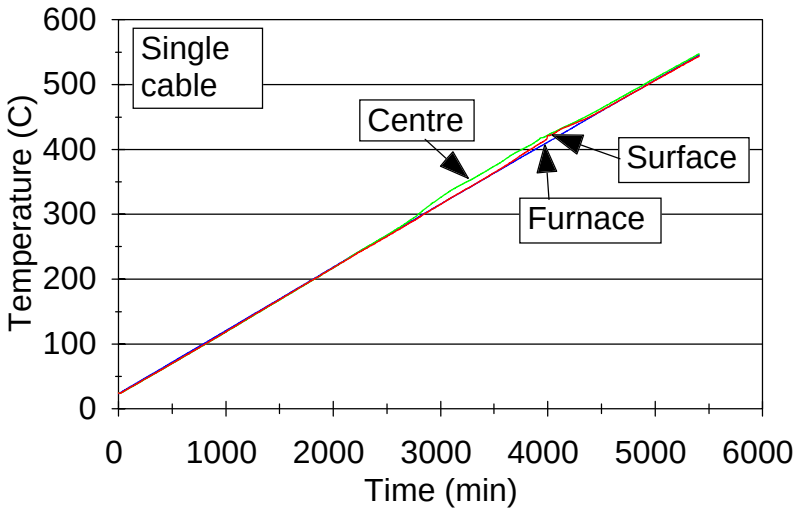

b)

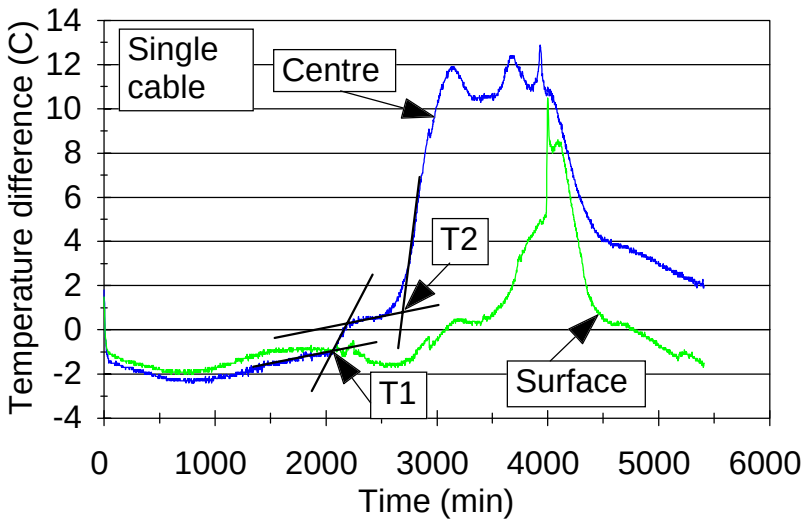

Figure 1. a) Temperatures in self-ignition test with one cable, b) difference between cable temperatures and furnace temperature. Straight lines on centre temperature curve demonstrate method of determining ignition temperatures T1 and T2.

a)

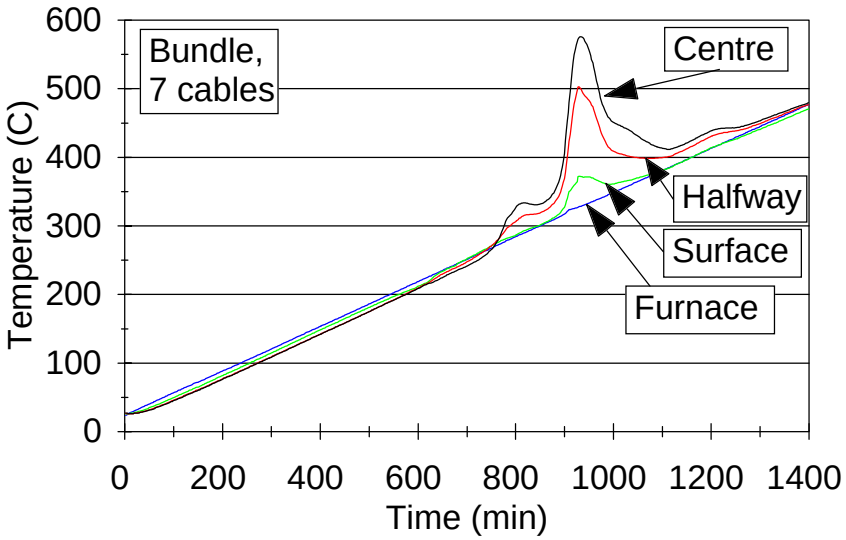

b)

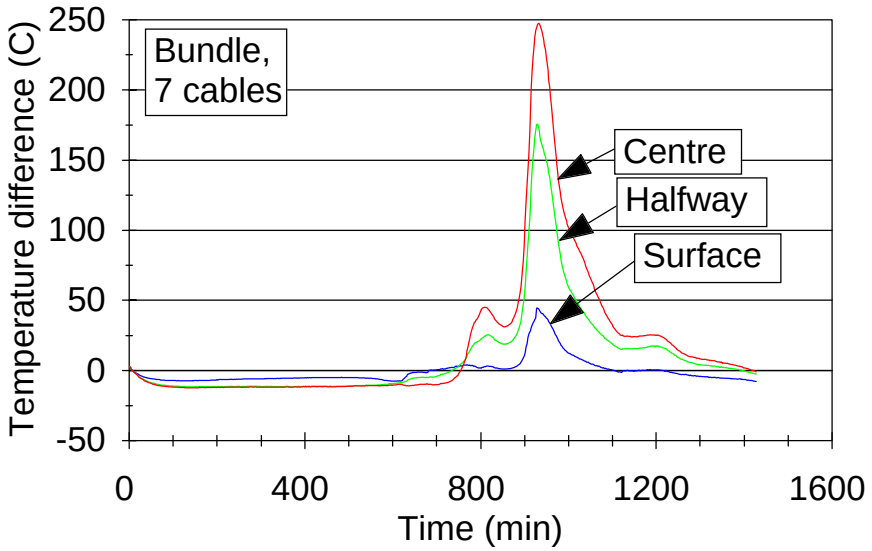

Figure 2. a) Temperatures in self-ignition test with bundle of 7 cables, b) difference between cable temperatures and furnace temperature.

a)

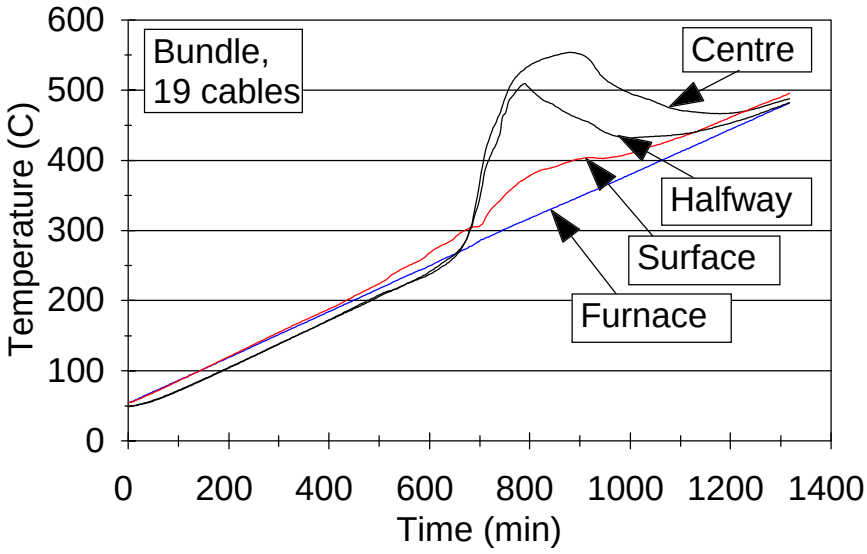

b)

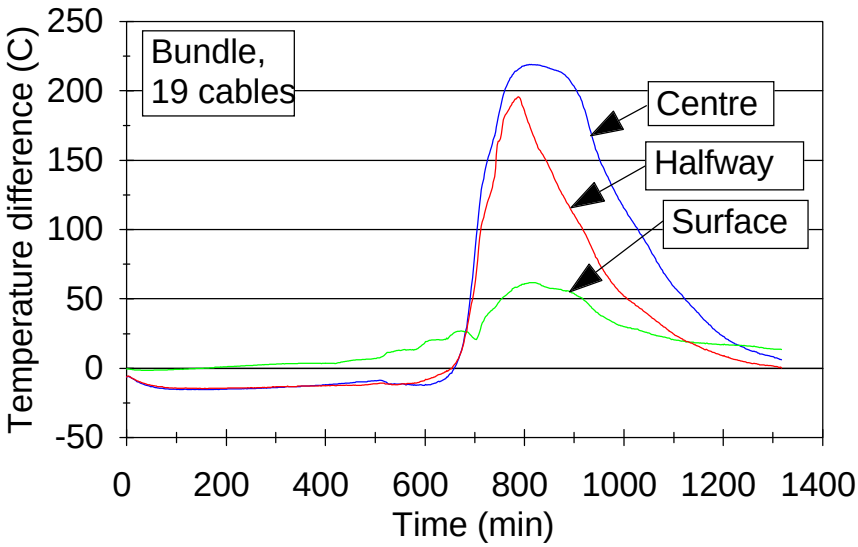

Figure 3. a) Temperatures in self-ignition test with bundle of 19 cables, b) difference between cable temperatures and furnace temperature.